

UCLA

UCLA Electronic Theses and Dissertations

Title

Engineering T cells to improve the efficacy and safety of adoptive T-cell therapy

Permalink

<https://escholarship.org/uc/item/8w23t76z>

Author

Nam, Eunwoo

Publication Date

2021

Peer reviewed|Thesis/dissertation

UNIVERSITY OF CALIFORNIA

Los Angeles

Engineering T cells to improve the efficacy and safety of
adoptive T-cell therapy

A thesis submitted in partial satisfaction
of the requirements for the degree Master of Science
in Chemical Engineering

by

Eunwoo Nam

2021

ABSTRACT OF THE THESIS

Engineering T cells to improve the efficacy and safety of
adoptive T-cell therapy

by

Eunwoo Nam

Master of Science in Chemical Engineering

University of California, Los Angeles, 2021

Professor Panagiotis D. Christofides, Chair

Adoptive T-cell therapy utilizing chimeric antigen receptors (CARs) has shown multiple successes in treating certain hard-to-treat blood cancers, leading to five CAR T-cell therapies approved by the FDA for leukemia, lymphoma, and multiple myeloma. Despite such successes, there remain several obstacles including antigen escape and severe T-cell mediated toxicities that limit the widespread implementation of the therapy. To address these challenges, we engineered and systematically optimized bispecific BCMA/CS1 CAR-T cells that recognize tumor cells if the target expresses either BCMA or CS1, thus effectively preventing antigen escape for multiple myeloma. Furthermore, we engineered self-regulating CD19 CAR-T cells that secrete cytokine modulators, which can neutralize inflammatory cytokines at the site of activated T cells, to effectively prevent cytokine release syndrome intrinsically and promptly. Taken together, we

ultimately seek to improve the efficacy and safety of CAR-based adoptive-T cell therapy to broaden the application of the therapy and provide effective cancer treatment.

The thesis of Eunwoo Nam is approved.

Philippe Sautet

Harold G. Monbouquette

Panagiotis D. Christofides, Committee Chair

University of California, Los Angeles

2021

TABLE OF CONTENTS

Abstract of the Thesis.....	ii
List of Figures.....	vi
List of Tables.....	vi
Acknowledgements.....	vii
Chapter 1: Introduction.....	1
Chapter 2: Investigation of ways to improve in vivo performance of BCMA/CS1 bispecific CAR-T cells to treat multiple myeloma.....	7
Chapter 3: Engineering self-regulating T cells to prevent cytokine release syndrome in CAR T-cell therapy.....	27

LIST OF FIGURES

- Figure 2.1. Lentivirally transduced CAR-T cells outperform HDR-modified CAR-T cells *in vitro*.
- Figure 2.2. Combination therapy with anti-PD-1 increases initial anti-tumor efficacy but not durability of response *in vivo*.
- Figure 2.3. BCMA/CS1 OR-gate CAR-T cells can eradicate solid tumor nodules *in vivo*.
- Figure 2.4. BCMA/CS1 OR-gate CAR-T cells achieve long-term persistence and prevents tumor relapse *in vivo*.
- Figure 3.1. Schematics of self-modulating CD19 CAR constructs.
- Figure 3.2. CD19 CAR-T cells can robustly co-express cytokine modulators without compromising CAR expression *in vitro*.
- Figure 3.3. Cytokine modulators neutralize signaling of their intended targets.
- Figure 3.4. Co-expression of cytokine modulators with CD19 CAR does not compromise T-cell function.
- Figure 3.5. CD19 CAR T cells induce CRS in humanized NSG-SGM3 mice.
- Figure 3.6. CD19 CAR T cells expressing tocilizumab scFv exhibit robust *in vivo* anti-tumor efficacy while reducing CRS-related toxicity.
- Figure 3.7. Tocilizumab scFv alters gene expression profile of CD19 CAR-T cells *in vivo*.

LIST OF TABLES

- Table 3.1. List of cytokine modulators tested in this study.

ACKNOWLEDGEMENTS

This research was conducted in collaboration with previous doctoral students Eugenia Zah (Chapter 2) and Meng-Yin Lin (Chapter 3) under the supervision of principle investigator Yvonne Y. Chen.

Chapter 2 is a modified version of the work published as an Open Access: Zah E, Nam E, Bhuvan V, Tran U, Ji BY, Gosliner SB, Wang X, Brown CE, Chen YY. Systematically optimized BCMA/CS1 bispecific CAR-T cells robustly control heterogeneous multiple myeloma. *Nature Communications*. 2020 May; 11(1):2283.

For Chapter 3, MYL built and evaluated the self-modulating CD19 CAR constructs, identified and optimized the humanized NSG-SGM3 mouse model for cytokine release syndrome, and assisted the design of the majority of experiments described. Select experiments and data analyses, represented by Figures 3.1, 3.3c,d, and 3.5, were performed by MYL.

This work was supported by grants from the Parker Institute for Cancer Immunotherapy awarded to Yvonne Y. Chen.

Chapter 1: Introduction

Adoptive T-cell therapy is a cancer treatment strategy that involves isolation of T cells from a patient's blood, genetic modification to express tumor-targeting receptors, *ex vivo* expansion, and re-infusion of the modified T cells back into the patient to treat the cancer. The development of chimeric antigen receptors (CARs), which are synthetic antigen receptors engineered to recognize tumor-associated antigens that are hardly targeted by natural T-cell receptors (TCRs), has broadened the potential clinical applications of adoptive T-cell therapy. This approach has demonstrated remarkable successes, particularly in treatment of relapsed or refractory CD19-expressing B-cell malignancies, with up to 90% complete remission rates, leading to the approval of the two CD19 CAR-T cell products by the United States Food and Drug Administration (FDA) in 2017, highlighting the potential of adoptive T-cell therapy as a new paradigm in treating previously untreatable cancers¹⁻⁸.

Chimeric antigen receptor (CAR) T-cell therapy

Chimeric antigen receptor is a recombinant receptor consisting of an antibody-derived single-chain variable fragment (scFv) that recognizes an antigen, an extracellular spacer, a transmembrane domain, and one or more signaling domains including the CD3 zeta chain. Adoptive T-cell therapy utilizing CARs has shown multiple successes in treating certain hard-to-treat blood cancers¹⁻⁸. Thus far, the FDA has approved five CAR T-cell therapies against leukemia, lymphoma, and multiple myeloma. However, despite such successes with adoptive CAR T-cell therapy, there remain several obstacles, such as antigen escape and severe T-cell mediated toxicities, that limit the widespread implementation of the therapy⁹.

Antigen escape in CAR T-cell therapy against multiple myeloma (MM)

Antigen escape occurs when tumor cells become resistant to adoptive T-cell therapy by eliminating the antigen targeted by T cells. Multiple myeloma (MM) is a cancer of plasma cells, which are defined to be terminally differentiated B cells. In recent years, administration of immunomodulatory drugs and proteasome inhibitors like thalidomide, lenalidomide, and bortezomib, in conjunction with autologous stem-cell transplant have greatly improved survival of patients from MM; however, MM remains an incurable disease^{10,11}. As plasma cells highly express B-cell maturation antigen (BCMA), the adoptive T-cell therapy with CAR-T cells targeting BCMA has been investigated and shown clinical efficacy against MM, achieving 80-100% response rate across multiple clinical trials¹²⁻¹⁶. However, clinical trial reports have also highlighted multiple cases of BCMA downregulation by MM cells after BCMA CAR T-cell treatment, resulting in tumor persistence or relapse^{12,13,15}. These results indicate that antigen escape is a significant limitation in the treatment of MM with BCMA CAR T-cell therapy. To address the problem of antigen escape with the BCMA CAR, we have developed bispecific CARs that simultaneously target both BCMA and CS1, which is another antigen that is highly expressed by the MM cells, and demonstrated that the bispecific CARs are able to robustly control MM tumor that are heterogeneous in antigen expression, while the single-input BCMA or CS1 CAR did not¹⁷. However, from the *in vivo* study, the majority of mice treated with bispecific CAR-T cells eventually succumbed to tumor outgrowth. Hence, in this thesis, we investigate ways to improve the anti-tumor efficacy of the bispecific BCMA/CS1 CAR-T cells to effectively treat MM while preventing antigen escape *in vivo*.

Cytokine release syndrome (CRS) in CAR T-cell therapy

Cytokine release syndrome (CRS) is an inflammatory response syndrome observed in patients treated with various forms of immunotherapy, including CAR T-cell therapy, and is characterized by the rapid and dramatic elevation of inflammatory cytokines and immunomodulatory proteins¹⁸⁻²¹. CRS is typically treated by the administration of corticosteroids or cytokine antagonists. However, systemic administration of such immunomodulators requires high doses with its own associated side effects, and the decision of when to provide these pharmaceutical interventions can be highly subjective. Alternative methods such as engineering T cells to express suicide genes can potentially reverse CRS after it has occurred, but such killing-based methods would force the therapy to terminate. To prevent CRS without terminating CAR-T cell therapy, we developed self-regulating CD19 CAR-T cells that automatically secrete cytokine antagonists. In this thesis, we characterize the self-regulating CD19 CAR-T cells *in vitro* and demonstrate the potential of the system to ameliorate CRS *in vivo* without compromising the therapeutic efficacy.

References

1. Kalos, M. *et al.* T cells with chimeric antigen receptors have potent antitumor effects and can establish memory in patients with advanced leukemia. *Science Translational Medicine* **3**, (2011).
2. Porter, D. L., Levine, B. L., Kalos, M., Bagg, A. & June, C. H. Chimeric Antigen Receptor–Modified T Cells in Chronic Lymphoid Leukemia. *New England Journal of Medicine* **365**, (2011).
3. Kochenderfer, J. N. *et al.* B-cell depletion and remissions of malignancy along with cytokine-associated toxicity in a clinical trial of anti-CD19 chimeric-antigen-receptor-transduced T cells. *Blood* **119**, (2012).
4. Brentjens, R. J. *et al.* CD19-targeted T cells rapidly induce molecular remissions in adults with chemotherapy-refractory acute lymphoblastic leukemia. *Science Translational Medicine* **5**, (2013).
5. Grupp, S. A. *et al.* Chimeric Antigen Receptor–Modified T Cells for Acute Lymphoid Leukemia. *New England Journal of Medicine* **368**, (2013).
6. Davila, M. L. *et al.* Efficacy and toxicity management of 19-28z CAR T cell therapy in B cell acute lymphoblastic leukemia. *Science Translational Medicine* **6**, (2014).
7. Kochenderfer, J. N. *et al.* Chemotherapy-refractory diffuse large B-cell lymphoma and indolent B-cell malignancies can be effectively treated with autologous T cells expressing an anti-CD19 chimeric antigen receptor. *Journal of Clinical Oncology* **33**, (2015).
8. Maude, S. L. *et al.* Chimeric Antigen Receptor T Cells for Sustained Remissions in Leukemia. *New England Journal of Medicine* **371**, (2014).

9. Shah, N. N. & Fry, T. J. Mechanisms of resistance to CAR T cell therapy. *Nature Reviews Clinical Oncology* vol. 16 (2019).
10. Cowan, A. J. Global burden of multiple myeloma. *JAMA Oncol.* **98121**, (2018).
11. Moreau, P., Attal, M. & Facon, T. Frontline therapy of multiple myeloma. *Blood* **125**, (2015).
12. Ali, S. A. T cells expressing an anti-B cell maturation antigen chimeric antigen receptor cause remissions of multiple myeloma. *Blood* **128**, (2016).
13. Brudno, J. T cells genetically modified to express an anti-B cell maturation antigen chimeric antigen receptor cause remissions of poor-prognosis relapsed multiple myeloma. *J. Clin. Oncol.* **36**, (2018).
14. Berdeja, J. G. Durable clinical responses in heavily pretreated patients with relapsed/refractory multiple myeloma: Updated results from a multicenter study of bb2121 anti-Bcma CAR T cell therapy. *Blood* **130**, (2017).
15. Cohen, A. D. Safety and efficacy of B cell maturation antigen (BCMA)-specific chimeric antigen receptor T cells (CART-BCMA) with cyclophosphamide conditioning for refractory multiple myeloma (MM). *Blood* **130**, (2017).
16. Smith, E. L. Development and evaluation of a human single chain variable fragment (scFv) derived Bcma targeted CAR T cell vector leads to a high objective response rate in patients with advanced MM. *Blood* **130**, (2017).
17. Zah, E. *et al.* Systematically optimized BCMA/CS1 bispecific CAR-T cells robustly control heterogeneous multiple myeloma. *Nature Communications* **11**, (2020).
18. Xu, X. J. & Tang, Y. M. Cytokine release syndrome in cancer immunotherapy with chimeric antigen receptor engineered T cells. *Cancer Letters* vol. 343 (2014).

19. Brentjens, R., Yeh, R., Bernal, Y., Riviere, I. & Sadelain, M. Treatment of chronic lymphocytic leukemia with genetically targeted autologous t cells: Case report of an unforeseen adverse event in a phase i clinical trial. *Molecular Therapy* vol. 18 (2010).
20. Morgan, R. A. *et al.* Case report of a serious adverse event following the administration of t cells transduced with a chimeric antigen receptor recognizing ERBB2. *Molecular Therapy* **18**, (2010).
21. Teachey, D. T. *et al.* Cytokine release syndrome after blinatumomab treatment related to abnormal macrophage activation and ameliorated with cytokine-directed therapy. *Blood* **121**, (2013).

Chapter 2: Investigation of ways to improve *in vivo* performance of BCMA/CS1 bispecific CAR-T cells to treat multiple myeloma

Abstract

Clinical trials involving anti-B-cell maturation antigen (BCMA) chimeric antigen receptor (CAR) has shown promising result against multiple myeloma (MM)¹⁻⁵. However, BCMA downregulation by MM cells after CAR T-cell treatment has been observed^{1,2,4}. These results indicate that antigen escape is limiting the efficacy of the treatment of MM with BCMA CAR T-cell therapy. To address the challenge of antigen escape, we generated several bispecific BCMA/CS1 CAR constructs using different combinations of BCMA- and CS1-targeting single-chain variable fragments (scFvs) and demonstrated that bispecific BCMA/CS1 CAR-T cells show superior control of heterogeneous MM tumor cells *in vivo* and prolonged animal survival compared to single-input BCMA or CS1 CAR-T cells⁶. However, despite the clear improvement in median survival, the majority of animals treated with bispecific CAR-T cells eventually succumbed to tumor outgrowth. Thus, we investigated various ways, including altering CAR T-cell manufacturing procedure or combining the therapy with a checkpoint inhibitor, to enhance the anti-tumor efficacy of bispecific BCMA/CS1 CAR-T cells *in vivo* while preventing antigen escape. Taken together with our previous work, we thoroughly outlined systematic optimization process of engineering CARs to treat cancers that currently lack effective treatment options.

Introduction

Multiple myeloma (MM) is the second-most common hematologic malignancy, causing 98,437 deaths globally in 2016, with an estimated 32,110 new diagnoses in the US in 2019^{7,8}. In recent years, immunomodulatory drugs and proteasome inhibitors such as thalidomide, lenalidomide, and bortezomib, which may be administered in conjunction with autologous stem-cell transplant, have substantially improved survival of patients suffering from MM⁹. However, MM remains an incurable disease despite these therapeutic options.

The adoptive transfer of CAR-T cells targeting B-cell maturation antigen (BCMA) has shown clinical efficacy against MM, achieving 80%–100% overall response rate across multiple clinical trials^{1–5}. However, BCMA is not uniformly expressed on MM cells, as evidenced by a recent study that screened 85 MM patients and found 33 to be BCMA negative¹, thus limiting patient eligibility for BCMA CAR T-cell therapy. Furthermore, multiple cases of patient relapse involving tumor cells with downregulated BCMA expression have been reported^{1,2,4}, underscoring antigen escape as a significant obstacle in the treatment of MM with BCMA CAR T-cell therapy. In addition, a substantial fraction of patients treated with BCMA CAR-T cells eventually relapse even when BCMA expression is retained^{1,2,4}, suggesting a lack of durable effector function by the engineered T cells.

To address the challenge of MM cells undergoing antigen escape upon BCMA CAR T-cell therapy, we developed bispecific CARs that target both BCMA and CS1 in a Boolean OR-gate logic function, such that T cells expressing the bispecific CARs can recognize target cells as long as the target cells express either BCMA or CS1⁶. This “OR-gate” bispecific CAR design can lower the probability of antigen escape because even if the MM cells lose one antigen, they would be still targetable by the CAR-T cells via the second target antigen. The CAR constructs

were rationally designed based on information such as size and binding-epitope location of the target antigens and using different combinations of BCMA- and CS1-targeting single-chain variable fragments (scFvs).

Then, the panel of CAR constructs were systematically tested *in vitro* for anti-tumor functions such as target-cell lysis, cytokine production, and T-cell proliferation upon antigen stimulation. Based on these high-throughput *in vitro* functionality assays, we then identified the two top-performing constructs and subsequently evaluated them *in vivo* against MM cells with heterogeneous antigen expression. From the *in vivo* study, based on tumor control and animal survival, we identified the best-performing construct, “huLuc63-c11D5.3 Short” (the bispecific CAR with huLuc63 scFv and c11D5.3 scFv connected by a short spacer)⁶. However, despite the clear improvement in median survival, the majority of animals treated with bispecific CAR-T cells eventually succumbed to tumor outgrowth⁶. In this thesis, we investigate various ways to enhance the anti-tumor efficacy of bispecific BCMA/CS1 CAR-T cells *in vivo* and build upon our proposed process of designing and optimizing new CARs. We demonstrate that virally integrated CARs outperform gene-edited counterparts; and demonstrate that combination therapy with anti-PD-1 antibody increases the speed of initial *in vivo* tumor clearance by BCMA/CS1 OR-gate CAR-T cells against established MM, but OR-gate CAR-T cells alone are sufficient to eradicate high tumor burdens, albeit over a longer time period, leading to effective and durable control of highly aggressive tumors.

Results

Virally integrated CARs outperform gene-edited counterparts

Having identified the lead OR-gate CAR candidate through *in vivo* testing⁶, we next evaluated whether alternative manufacturing processes may further bolster T-cell function. It had been reported that CAR-T cells with the CAR integrated into the T-cell receptor α constant (TRAC) locus via homology-directed repair (HDR) exhibit longer T-cell persistence and less exhaustion upon antigen stimulation *in vivo* compared to retrovirally transduced CAR-T cells¹⁰. It was hypothesized that the endogenous gene-expression regulation machinery of the TRAC locus enabled dynamic regulation of CAR expression, leading to superior functional output¹⁰. We thus integrated the FLAG-tagged OR-gate CAR into the TRAC locus (Fig. 2.1a) and verified TRAC knock-out and CAR knock-in by surface antibody staining for TCR α/β chains and the FLAG-tag, respectively (Fig. 2.1b).

Consistent with previous report, CAR expression from the TRAC locus was lower than that detected in virally transduced cells (Fig. 2.1c)¹⁰. TRAC-knockout T cells showed comparable viability to that of lentivirally transduced cells, indicating CRISPR/Cas9-mediated editing through RNP nucleofection did not compromise cell viability (Fig. 2.1d). However, contrary to expectations, TRAC-knockout T cells that were HDR-modified to express the OR-gate CAR showed poor viability and inferior cytotoxicity upon repeated antigen challenge compared to lentivirally transduced OR-gate CAR-T cells (Fig. 2.1d,e). Furthermore, HDR-modified cells showed weaker antigen-stimulated T-cell proliferation (Fig. 2.1f), as well as higher and more durable exhaustion-marker expression (Fig. 2.1g), compared to lentivirally transduced cells. These results suggest that whether site-specific CAR integration into the TRAC locus is beneficial to T-cell function may depend on the specific CAR construct involved. Based

on these findings, lentiviral transduction was retained as the preferred method for CAR T-cell generation.

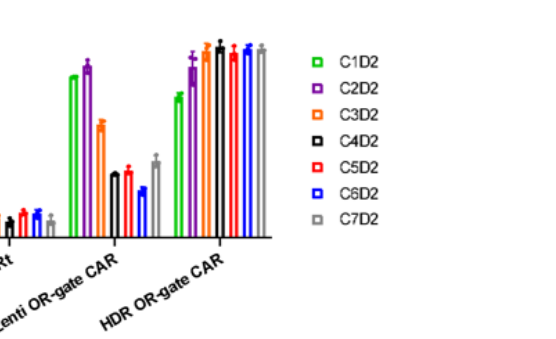
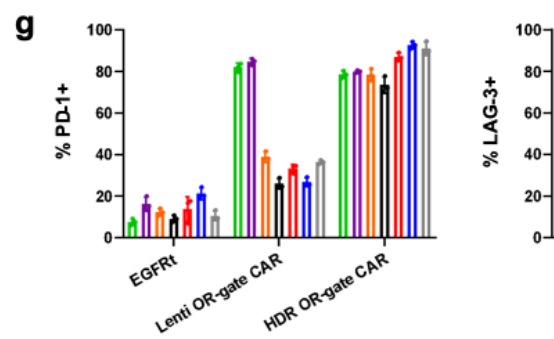
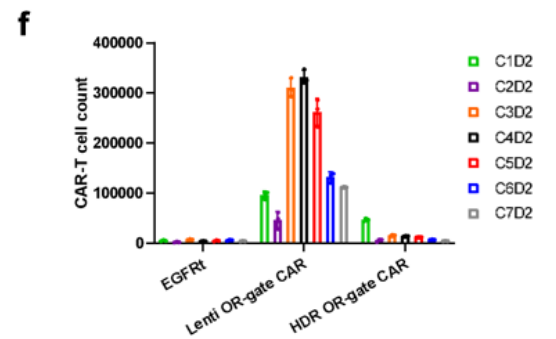
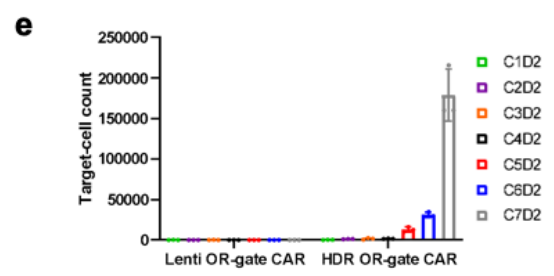
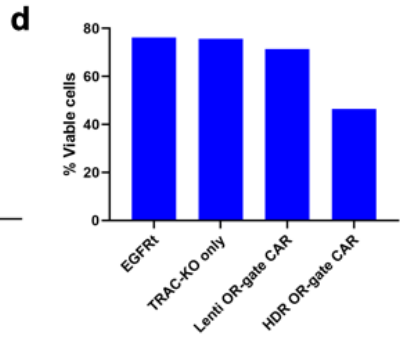
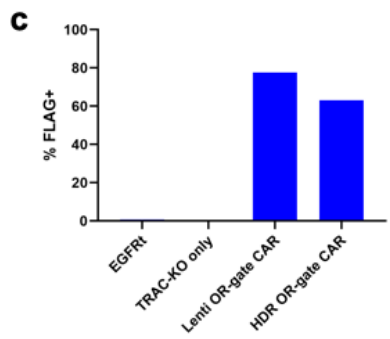
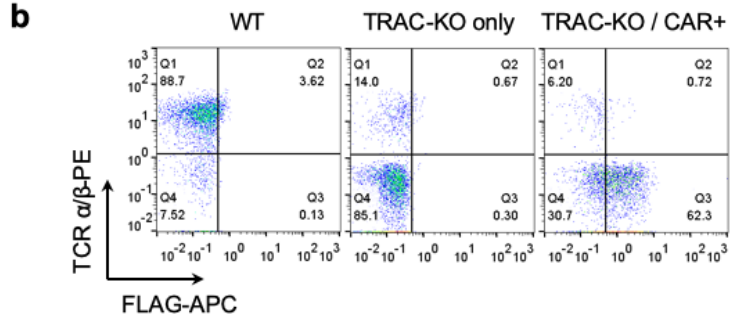


Fig. 2.1. Lentivirally transduced CAR-T cells outperform HDR-modified CAR-T cells *in vitro*. (a) Schematic of an AAV vector encoding homology arms (left and right, LHA and RHA) flanking an integration cassette consisting of a splice-acceptor (SA) site, a T2A sequence, and the FLAG-tagged huLuc63-c11D5.3 OR-gate CAR. (b) Representative TCR α/β and FLAG-tag flow plots 11 days post RNP nucleofection and AAV transduction. (c) HDR-modified T cells exhibit lower CAR surface expression than lentivirally-transduced T cells. (d) HDR-modified OR-gate CAR-T cells exhibit relatively poor viability 11 days post RNP nucleofection/AAV transduction. (e–g) Upon repeated antigen challenge with WT MM.1S cells, HDR-modified OR-gate CAR-T cells exhibit (e) inferior cytotoxicity, (f) weaker antigen-stimulated T-cell proliferation, and (g) stronger and longer-lasting exhaustion-marker (PD-1 and LAG-3) expression than lentivirally transduced OR-gate CAR-T cells. Values shown are the mean of technical triplicate samples with error bars indicating ± 1 SD. Results shown are representative of cells generated from two healthy donors.

Bispecific CAR T-cell and anti-PD-1 combination therapy

Tissue recovered at the time of animal sacrifice in the previous *in vivo* study revealed the presence of CAR-T cells, but they were generally present at low frequency and with high PD-1 expression⁶. This observation suggested combination therapy with checkpoint inhibitors may improve treatment efficacy. Indeed, we found that co-administration of anti-PD-1 antibody and the OR-gate CAR-T cells led to more effective tumor control compared to OR-gate CAR-T cells alone at early time points. By day 48 post T-cell injection (day 56 post tumor injection), 5/6 animals treated with OR-gate CAR-T cells plus anti-PD-1 exhibited complete tumor clearance, compared to 1/6 animal in the group treated with CAR-T cells alone (Fig. 2.2a). The beneficial effect of checkpoint inhibition was dependent on the presence of CAR-T cells, as anti-PD-1 therapy alone or in combination with mock-transduced T cells did not confer anti-tumor capability. In fact, the addition of anti-PD-1 antibodies appeared to reduce the allogeneic effect exerted by mock-transduced T cells on engrafted tumors (Fig. 2.2a).

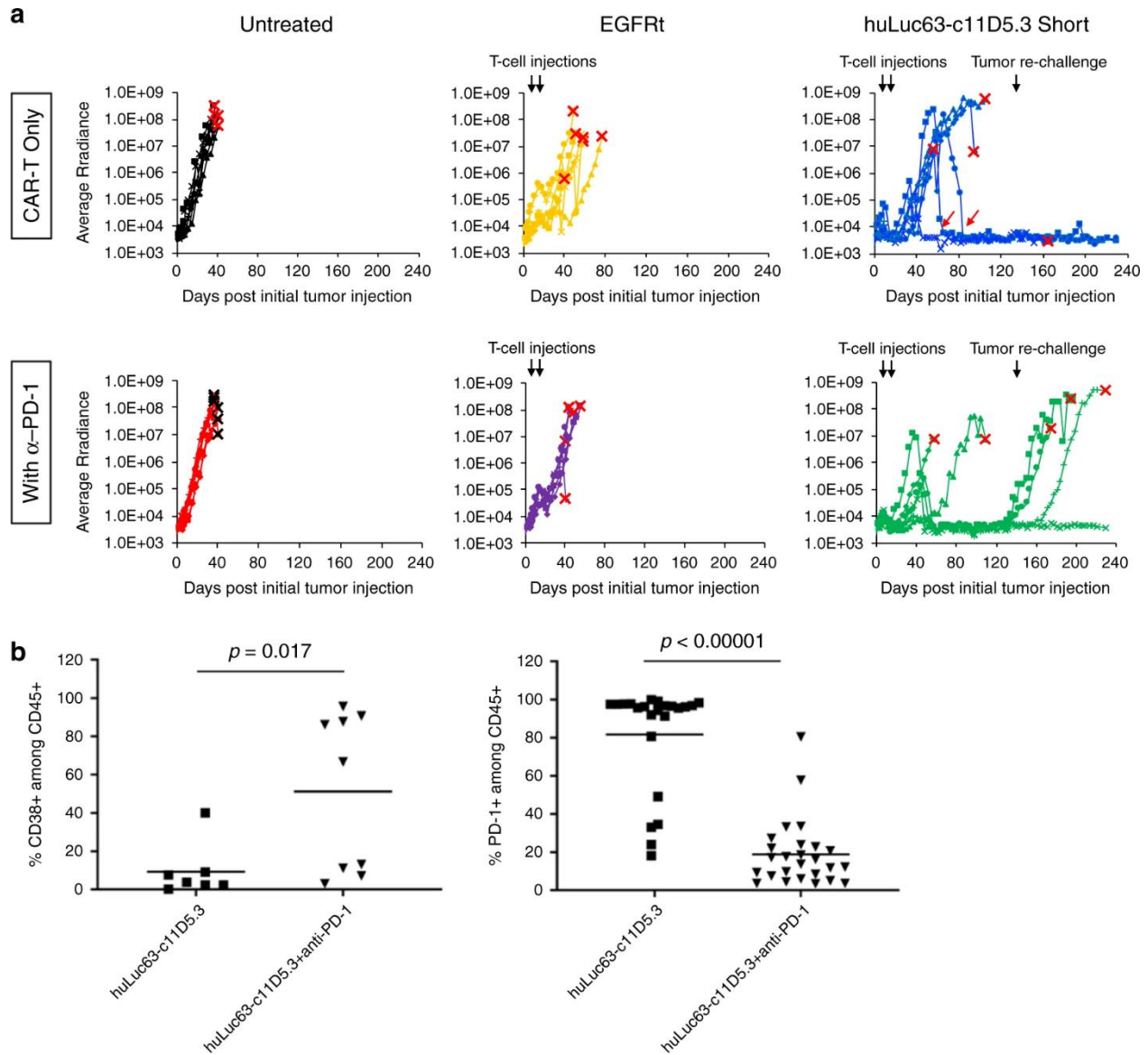
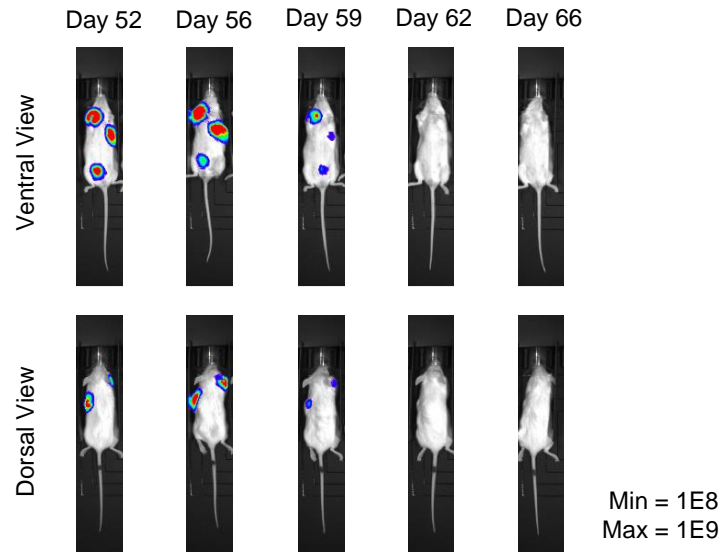


Fig. 2.2. Combination therapy with anti-PD-1 increases initial anti-tumor efficacy but not durability of response *in vivo*. (a) Mice were engrafted with 1.5×10^6 WT MM.1S cells. Tumor-bearing animals were treated with 1.5×10^6 EGFRt- or CAR-expressing T cells on day 8 (8 days after tumor injection) and day 16. Tumor progression was monitored by bioluminescence imaging and shown for individual animals in each test group ($n = 6$). On day 133, animals that had been tumor-free for at least 7 weeks (3 each in the huLuc63-c11D5.3 Short groups with and without anti-PD-1) were re-challenged with 1.5×10^6 WT MM.1S cells. Black arrows indicate time of cell injections; red arrows indicate instances of CAR-T cells eradicating palpable tumor nodules. The endpoint for each animal is marked with an "X." (b) CD38 and PD-1 expression on T cells persisting in mice at time of animal sacrifice. Each data point corresponds to an individual tumor mass, tissue (e.g., brain and spleen), or cardiac blood sample recovered that

included at least 10 CD45+ cells as detected by flow cytometry. P values were calculated by unpaired two-tailed Student's t-test; n.s. not statistically significant ($p > 0.05$); * $p < 0.05$; ** $p < 0.01$.

Although CAR-T cell treatment alone failed to control initial tumor progression in most animals, two mice that had developed palpable solid tumors became tumor free 50 and 68 days after the second and final T-cell infusion, respectively (red arrows in Fig. 2.2a; Fig. 2.3). This result demonstrates BCMA/CS1 OR-gate CAR-T cells' ability to eradicate established solid-tumor masses even after a prolonged period *in vivo*. Notably, all animals that achieved complete tumor clearance in the "CAR-T only" treatment group remained tumor free over the entire study duration, even after tumor re-challenge performed on day 133 (117 days after the second and last T-cell infusion, Fig. 2.2a). One of the animals in this group was sacrificed on day 165 of the study due to symptoms consistent with graft versus host disease, in the complete absence of tumor signal (Fig. 2.4a).

Mouse #1 of huLuc63-c11D5.3 Short CAR-T Only Group



Mouse #3 of huLuc63-c11D5.3 Short CAR-T Only Group

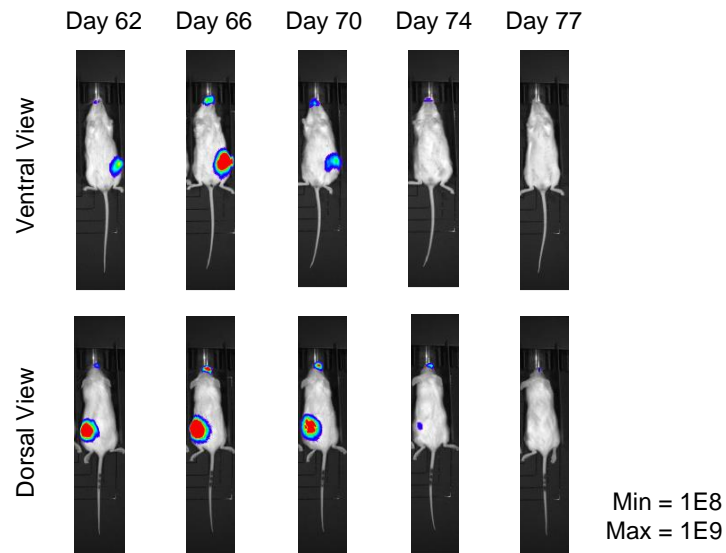


Fig. 2.3. BCMA/CS1 OR-gate CAR-T cells can eradicate solid tumor nodules *in vivo*. NSG mice were engrafted with MM.1S tumors and treated with BCMA/CS1 OR-gate CAR-T cells as described in Fig. 2.2. Two animals in the group treated with huLuc63-c11D5.3 Short CAR-T cells without anti-PD-1 developed palpable solid tumor nodules in the chest and flank, but the tumors eventually regressed to below detection levels and the animals have remained viable in a tumor-free state for >20 weeks, including after tumor re-challenge on day 133, until the study

was terminated on day 229. Bioluminescence imaging of the animals in dorsal and ventral views are shown.

In a surprise finding, animals treated with OR-gate CAR-T cells plus anti-PD-1 showed a higher rate of relapse at later time points compared to those treated with CAR-T cells alone. Specifically, two out of five animals that achieved initial tumor clearance experienced relapse before the time of tumor re-challenge, and another two failed to prevent tumor outgrowth after re-challenge (Fig. 2.2a). Verma et al. recently reported that PD-1 blockade in suboptimally primed T cells can induce a dysfunctional PD-1⁺/CD38⁺ population, resulting in decreased anti-tumor efficacy¹¹. In our study, animals were given twice-weekly injections of anti-PD-1 even after they have achieved tumor clearance, thus the CAR-T cells may have become dysfunctional due to continual exposure to anti-PD-1 in the absence of antigen stimulation. Consistent with this hypothesis, we found a higher frequency of CD38⁺ cells among T cells recovered from animals treated with anti-PD-1 (Fig. 2.2b). T cells harvested from this group of animals also showed significantly lower PD-1 staining. However, this may be due to the fact that the PD-1 molecules are already masked by the anti-PD-1 antibodies administered to the animals. (Clone EH12.2H7 was used for mouse treatment; clone PD1.3.1.3 was used for flow cytometry analysis after T-cell recovery. Zelba et al. reported that both EH12.2H7 and PD1.3.1.3 compete with pembrolizumab for antigen binding, suggesting that the three monoclonal antibodies all bind to overlapping epitopes¹².) Taken together, these results suggest that administration of anti-PD-1 could accelerate tumor clearance at early time points and increase the initial rate of response, but prolonged anti-PD-1 administration may not provide added benefits to BCMA/CS1 CAR-T cell therapy. Large-scale animal studies that track animal response over an extended time period would be advisable before ascertaining the benefit of combination immunotherapies.

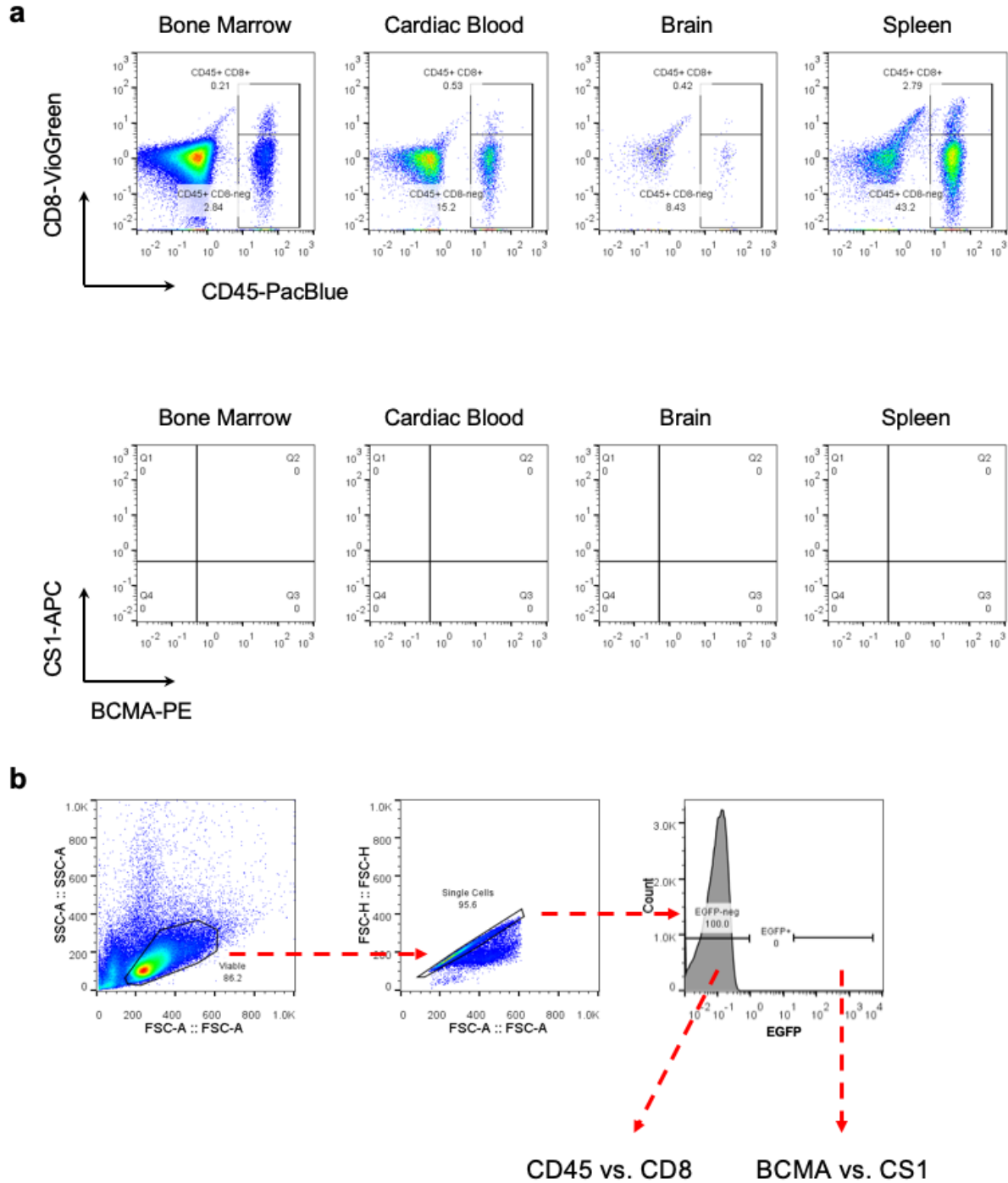


Fig. 2.4. BCMA/CS1 OR-gate CAR-T cells achieve long-term persistence and prevents tumor relapse *in vivo*. (a) In the experiment shown in Fig. 2.2, an animal in the huLuc63-c11D5.3 Short CAR-T cell-treated group without anti-PD-1 was sacrificed on day 165 due to severe weight loss despite the complete absence of tumor signal. This animal had been showing signs of graft-versus-host disease, including fur loss and skin inflammation, for approximately 13 weeks prior to the endpoint. At the time of sacrifice, bone marrow, cardiac blood, brain, and

spleen tissue were collected and analyzed by flow cytometry for signs of human T cells and MM.1S tumor cells. Results indicate robust persistence of T cells and the complete absence of tumor cells in this animal. (b) Gating strategy for data shown in (a).

Discussion

In this study, we found that lentivirally transduced CAR-T cells exhibit greater anti-tumor activity compared to CAR-T cells generated through CRISPR/Cas9-mediated editing (Fig. 2.1). This finding was unexpected given the compelling data from a previous study demonstrating functional superiority of T cells that had undergone site-specific integration of the CAR transgene into the TRAC locus¹⁰. Our findings suggest that further exploration may be warranted to determine whether the benefit of site-specific CAR transgene integration is limited to some CARs and, if so, whether the difference is determined by the antigen specificity of the CAR or more generalizable properties such as the size of the CAR construct (and thus the size of the HDR template).

Multiple ongoing clinical trials are investigating the effect of combining CAR-T cell therapy with checkpoint inhibitors (e.g., NCT04003649, NCT00586391, NCT03726515), reflecting interest in the field to explore synergy between these two potent therapeutic paradigms. We demonstrated that the co-administration of anti-PD-1 antibody with OR-gate CAR-T cells can accelerate the rate of initial tumor eradication in animals that had been engrafted with highly aggressive MM xenografts, but continued anti-PD-1 administration may not provide added benefits in the long run (Fig. 2.2). A recent study reported that PD-1 blockade actually induces dysfunction in sub-optimally primed T cells¹¹. In our study, anti-PD-1 treatment showed clear beneficial effects at early time points, when tumor burden was still present. After day 60, the vast majority of OR-gate CAR-T cell-treated animals had achieved tumor-free status and thus ceased to provide antigen stimulation to T cells. It is plausible that continued

administration of anti-PD-1 induced T-cell dysfunction during the >2-month period between initial tumor clearance and tumor re-challenge on day 133, causing antibody-treated animals eventually failed to resist the second tumor challenge. Taken together, our findings suggest that combining CAR-T cell and checkpoint inhibitor therapies requires judicious examination of the timing and duration of the combination therapy, and an even larger-scale *in vivo* study would be warranted to clearly understand the effect of long-term administration of anti-PD-1 antibody after CAR-T cell therapy.

Here, each of CAR designs, T-cell functionality assays performed, and animal experiments performed may not be as novel; however, our proposed research does present an innovative solution for designing and engineering new CARs by outlining a systematic optimization process to improve upon current cancer treatment or to develop new treatment for other cancer types that currently lack effective treatment options.

Materials and Methods

Plasmid construction

Single-chain bispecific BCMA-OR-CS1 CARs were constructed by isothermal assembly¹³ of DNA fragments encoding the following components. BCMA-specific single-chain variable fragments (scFvs) were derived from the c11D5.3 monoclonal antibody (mAb)¹⁴. CS1-specific scFvs were derived from Luc90 or huLuc63 mAb¹⁵. Each CAR also contained an IgG4-based extracellular spacer, the CD28 transmembrane domain, and the cytoplasmic domains of 4-1BB and CD3 ζ . All CARs were fused to a truncated epidermal growth factor receptor (EGFRt) via a T2A peptide to facilitate antibody staining of CAR-expressing cells¹⁶. An N-terminal FLAG tag was also added to each CAR to enable quantification of CAR surface expression.

Cell-line generation and maintenance

MM.1S cells (ATCC) were lentivirally transduced to express the EGFP–firefly luciferase (ffLuc) fusion gene, and EGFP+ cells were enriched by fluorescence-activated cell sorting (FACS) to >98% purity. BCMA– or CS1– MM.1S cells were generated by CRISPR/Cas9-mediated gene knockout. MM.1S cells (5×10^6) were nucleofected with ribonucleoprotein (RNP), consisting of chemically synthesized gRNA (Synthego) targeting BCMA or CS1 complexed to purified Cas9 protein, using Ingenio Electroporation Solution (Mirus Bio) and the Amaxa Nucleofector 2B Device (Lonza) following manufacturers’ protocols. Four days after nucleofection, cells were surface-stained with BCMA-PE and CS1-APC antibodies (BioLegend) to verify antigen knockout. The cells were subsequently bulk-sorted for BCMA– or CS1– populations by fluorescence-activated cell sorting using a FACSAria (II) sorter at the UCLA Flow Cytometry Core Facility, and the sorted polyclonal population was expanded for use in *in vitro* and *in vivo* experiments. MM.1S cells were cultured in complete T-cell medium (RPMI-1640 (Lonza) with 10% heat-inactivated FBS (HI-FBS; Life Technologies)). HEK293T cells (ATCC) were cultured in DMEM (VWR) supplemented with 10% HI-FBS.

Lentivirus production

HEK 293T cells seeded in 10-cm dishes at 3.5×10^6 cells in 9 mL DMEM +10% HI-FBS media were transfected by linear PEI. Sixteen hours post-transfection, cells were washed with PBS and supplemented with fresh media containing 60 mM sodium butyrate (Sigma-Aldrich). Viral supernatant was collected 24 hours and 48 hours after media change, and cell debris was removed from the supernatant by centrifugation at $450 \times g$ for 10 min at 4°C, followed by filtration through a 0.45 μ M membrane (Corning). Viral supernatant collected 24 hours after

media change was mixed with 1/4 volume 40% polyethylene glycol 8000 (PEG) (Amresco) in 1X-PBS and rotated overnight at 4°C. PEG-treated virus was pelleted at 1,000 x g for 20 min at 4°C, then resuspended in viral supernatant collected 48 hours after media change, and finally ultracentrifuged at 51,300 x g for 1 hour and 35 minutes at 4°C. Pellets were resuspended in 200 µL of serum-free RPMI-1640 and then incubated for 1 hour at 4°C to allow complete dissolution. Virus was then stored at –80°C for subsequent titer and use.

Adeno-associated virus production

HEK 293T cells seeded in eighteen 10-cm dishes at 3×10^6 cells in 9 mL of DMEM + 10% HI-FBS media were transfected by linear PEI. After 72 hours, cells were harvested, pelleted at 1,000 x g for 5 minutes at 4°C, then resuspended in 14.4 mL of 50 mM Tris + 150 mM NaCl (pH 8.2). The cells were lysed by undergoing three freeze/thaw cycles, then incubated at 37°C for 1 hour with benzonase (10 U/mL; EMD Millipore). The lysate was then centrifuged at 13,200 x g for 10 minutes at room temperature. Supernatant was collected and stored at 4°C until next step. The lysate supernatant was ultracentrifuged with iodixanol (OptiPrep; StemCell Technologies) density gradient solutions (54%, 40%, 25%, and 15% w/v) at 76,900 x g for 18 hours at 4°C. Then, 4/5 of the 40% layer and 1/5 of the 54% layer were extracted from the polyallomer Quick-seal ultracentrifuge tube (Fisher) with an 18-gauge needle (Fisher) attached to a 10-mL syringe (VWR). The collected virus fraction was diluted in an equal volume of PBS + 0.001% Tween-20, applied to an Amicon Ultra-15 (EMD Millipore, 10 kDa NMWL) column, and centrifuged at 4,000 x g for 20 minutes at 4°C. The resulting virus fraction was diluted with PBS + 0.001% Tween-20 and centrifuged until 500 µL of the virus fraction remained in the column. Concentrated virus was stored at 4°C for subsequent titer and use.

Generation of CAR-expressing primary human T cells

CD25⁻/CD14⁻/CD62L⁺ “naïve/memory” (NM) T cells were isolated from healthy donor whole blood obtained from the UCLA Blood and Platelet Center. Peripheral mononuclear blood cells (PBMCs) were isolated using Ficoll density-gradient separation, and NM T cells were subsequently isolated from PBMCs using magnetism-activated cell sorting (Miltenyi) to first deplete CD25⁻ and CD14⁻ expressing cells and next enrich for CD62L⁺ cells. Isolated T cells were stimulated with CD3/CD28 T-cell activation Dynabeads (Life Technologies) at a 1:3 bead:cell ratio. T cells were lentivirally transduced 48 hours after stimulation at a multiplicity of infection of 1.5. Dynabeads were removed 7 days post stimulation. For CAR-T cells with CAR integrated via homology-directed repair (HDR), Dynabeads were removed 3 days post stimulation, and T cells were nucleofected with RNP, consisting of a previously reported single-guide RNA targeting the 5' end of exon 1 of T-cell receptor α constant (TRAC) locus¹⁰ complexed to purified Cas9 protein. Nucleofected cells were incubated at 37°C for 10 minutes, and then transduced with adeno-associated virus (AAV) at a multiplicity of infection of 3×10^5 . All T cells were expanded in complete T-cell medium and fed interleukin (IL)-2 (50 U/mL; Life Technologies) and IL-15 (1 ng/mL; Miltenyi) every 2–3 days. CAR-T cells were evaluated without further cell sorting.

Flow Cytometry

Flow cytometry in this study was performed with a MACSQuant VYB cytometer (Miltenyi Biotec). T-cells were assessed for surface presentation of epitopes using fluorophore-conjugated monoclonal antibodies for DYKDDDDK (also known as FLAG; BioLegend #637308, 1:250 dilution), PD-1 (Miltenyi #130-117-698, 1:100 dilution), LAG-3 (eBioscience #17-2239-42 or

BioLegend #369314, 1:100 dilution), CD45 (BioLegend #304022, 1:100 dilution), or TCR α/β (BioLegend #306704, 1:100 dilution). EGFRt expression was measured with Erbitux (Bristol-Myers Squibb) biotinylated in-house (EZ-link Sulfo-NHS-Biotin, Pierce, 1:100 dilution). For biotin-conjugated antibodies, PE-conjugated streptavidin (Jackson ImmunoResearch #016-110-084, 1:100 dilution) was used subsequently. Tumor cells were analyzed for antigen expression with APC-conjugated anti-CS1 antibody (BioLegend #331809, 1:50 dilution) or PE-conjugated anti-BCMA antibody (BioLegend #357503, 1:50 dilution). Flow data were analyzed and gated in FlowJo (TreeStar; see Supplementary Fig. 18 for an example of gating strategy). Unless otherwise noted, data shown are drawn from biological triplicates (i.e., three distinct samples).

Repeated antigen challenge

Target cells were seeded at $1.8\text{--}5 \times 10^5$ cells/well in a 48- or 24-well plate and coincubated with effector cells at an E:T ratio of 1:1 or 1:2 (1–1.5 ml total volume/well). Effector cell seeding was based on CAR⁺ T-cell count. Remaining target cells were quantified by flow cytometry every 2 days. Fresh target cells ($1.8\text{--}5 \times 10^5$ cells/well) were added to effector cells every 2 days after cell counting.

***In vivo* xenograft studies in NSG mice**

All *in vivo* experiments were approved by the UCLA Animal Research Committee (ARC). Six-to-eight-week-old male and female NSG mice were bred in house by the UCLA Department of Radiation and Oncology. Animals were housed in UCLA Division of Laboratory Animal Medicine (DLAM) facilities where temperature, humidity, and illumination were maintained according to ARC guidelines. EGFP⁺, ffLuc-expressing MM.1S cells ($1.5\text{--}2 \times 10^6$) were

administered to NSG mice via tail-vein injection. Upon confirmation of tumor engraftment (5–8 days post tumor cell injection), mice were treated with $0.5\text{--}1.5 \times 10^6$ EGFRt-transduced or CAR+/EGFRt+ cells via tail-vein injection. In some experiments, animals were re-dosed 8 days later with a second injection of 1.5×10^6 T cells as noted in the text and figure captions. Tumor progression was monitored by bioluminescence imaging using an IVIS Lumina III LT Imaging System (PerkinElmer), and images were collected and analyzed using Living Image Software version 4.4 (Perkin Elmer). For combination therapy with anti-PD-1, mice were treated with 200 μg of anti-PD-1 (Ultra-LEAF, BioLegend) via intraperitoneal (i.p.) injection every 3-4 days starting one day before T-cell injection. In the experiment to evaluate anti-PD-1, animals that had been tumor-free for at least 7 weeks were re-challenged with 1.5×10^6 EGFP+, ffLuc-expressing WT MM.1S cells via tail-vein injection on day 133. At the time of sacrifice, cardiac blood and tissue (e.g., brain, spleen, tumor mass) were collected for analysis. Prior to staining, cardiac blood was treated with Red Blood Cell Lysis Solution (Miltenyi) following manufacturer's protocol. Tissue was processed by cutting the sample finely with a surgical scissor, filtering through a 100 μm cell strainer (Corning), and then washing with PBS.

Statistical analysis

Statistical significance of *in vitro* results was analyzed using two-tailed, unpaired, Student's t-test with Bonferroni correction for multiple comparisons. Animal survival data were analyzed by log-rank analysis. All experiments were performed with biological replicates—i.e., measurements were taken from distinct samples.

References

1. Ali, S. A. T cells expressing an anti-B cell maturation antigen chimeric antigen receptor cause remissions of multiple myeloma. *Blood* **128**, (2016).
2. Brudno, J. T cells genetically modified to express an anti-B cell maturation antigen chimeric antigen receptor cause remissions of poor-prognosis relapsed multiple myeloma. *J. Clin. Oncol.* **36**, (2018).
3. Berdeja, J. G. Durable clinical responses in heavily pretreated patients with relapsed/refractory multiple myeloma: Updated results from a multicenter study of bb2121 anti-Bcma CAR T cell therapy. *Blood* **130**, (2017).
4. Cohen, A. D. Safety and efficacy of B cell maturation antigen (BCMA)-specific chimeric antigen receptor T cells (CART-BCMA) with cyclophosphamide conditioning for refractory multiple myeloma (MM). *Blood* **130**, (2017).
5. Smith, E. L. Development and evaluation of a human single chain variable fragment (scFv) derived Bcma targeted CAR T cell vector leads to a high objective response rate in patients with advanced MM. *Blood* **130**, (2017).
6. Zah, E. *et al.* Systematically optimized BCMA/CS1 bispecific CAR-T cells robustly control heterogeneous multiple myeloma. *Nature Communications* **11**, (2020).
7. American Cancer Society. Cancer Facts and Figures 2019. *American Cancer Society* (2019).
8. Cowan, A. J. Global burden of multiple myeloma. *JAMA Oncol.* **98121**, (2018).
9. Moreau, P., Attal, M. & Facon, T. Frontline therapy of multiple myeloma. *Blood* **125**, (2015).

10. Eyquem, J. Targeting a CAR to the TRAC locus with CRISPR/Cas9 enhances tumour rejection. *Nature* **543**, (2017).
11. Verma, V. PD-1 blockade in subprimed CD8 cells induces dysfunctional PD-1+CD38hi cells and anti-PD-1 resistance. *Nat. Immunol.* **20**, (2019).
12. Zelba, H. Accurate quantification of T-cells expressing PD-1 in patients on anti-PD-1 immunotherapy. *Cancer Immunol. Immunother.* **67**, (2018).
13. Gibson, D. G. Enzymatic assembly of DNA molecules up to several hundred kilobases. *Nat. Methods* **6**, (2009).
14. Carpenter, R. O. B cell maturation antigen is a promising target for adoptive T-cell therapy of multiple myeloma. *Clin. Cancer Res.* **19**, (2013).
15. Chu, J. Genetic modification of T cells redirected toward CS1 enhances eradication of myeloma cells. *Clin. Cancer Res.* **20**, (2014).
16. Wang, X. A transgene-encoded cell surface polypeptide for selection, in vivo tracking, and ablation of engineered cells. *Blood* **118**, (2011).

Chapter 3: Engineering self-regulating T cells to prevent cytokine release syndrome in CAR T-cell therapy

Abstract

Cytokine release syndrome (CRS) is an inflammatory response syndrome observed in patients treated with various forms of immunotherapy and is characterized by the rapid and dramatic elevation of inflammatory cytokines and immunomodulatory proteins¹⁻⁴. CRS is commonly treated by the administration of corticosteroids, which suppress inflammatory responses, and tocilizumab, an antagonistic antibody targeting IL-6R α ⁵. However, both corticosteroids and tocilizumab require high dose administration, which does not localize the immunomodulators to the site of activated T cells and may lead to unwanted side effects. As such, to prevent CRS, we developed cytokine antagonists in a single-chain variable fragment (scFv) form, which are derived from their antibody structure, and engineered CAR-T cells to secrete the cytokine antagonists so that the secreted cytokine antagonists would neutralize their target CRS-related cytokines at the site of activated T cells. This thesis describes the *in vitro* characterization of the self-regulating CD19 CAR-T cells and demonstrates the potential of self-regulating CAR-T cells to prevent CRS *in vivo* without compromising their therapeutic efficacy.

Introduction

Adoptive T-cell therapy is a cancer treatment strategy that involves isolation of T cells from a patient's blood, genetic modification to express tumor-targeting receptors, *ex vivo* expansion, and re-infusion of the modified T cells back into the patient to treat the cancer. The

development of chimeric antigen receptors (CARs), which are synthetic antigen receptors engineered to recognize tumor-associated antigens, has broadened the potential clinical applications of adoptive T-cell therapy. This approach has demonstrated remarkable successes in the treatment of relapsed or refractory CD19-expressing B-cell malignancies, with up to 90% complete remission rates⁶⁻¹³, leading to the approval of the two CD19 CAR-T cell products by the United States Food and Drug Administration (FDA) in 2017⁶⁻¹¹.

Despite its notable efficacy, CAR T-cell therapy is not yet a front-line treatment option for cancer in part due to the risk of severe treatment-related toxicities. One of the major challenges is cytokine release syndrome (CRS), which is a systemic inflammatory response often observed in patients treated with CD19 CAR-T cells and is characterized by the rapid and dramatic elevation of inflammatory cytokines and immunomodulatory proteins¹⁻⁴. CRS has also been reported for other CAR-T cell therapies targeting HER2, BCMA, and mesothelin^{3,14,15}, and severe CRS has been identified as the cause of death for multiple patients in clinical trials^{2,3}.

The clinical management of CRS commonly involves the administration of tocilizumab, an antagonistic antibody targeting interleukin 6 receptor alpha (IL-6R α), and corticosteroids, which non-specifically suppress inflammatory responses^{5,16}. Patients undergoing CRS tend to have high levels of IL-6, which could bind to soluble IL-6R α and form a ligand-receptor complex that can interact with membrane-bound gp130 and induce proinflammatory ‘trans-signaling’¹⁷. Tocilizumab binds both membrane-bound and soluble IL-6R α and prevents binding of IL-6 to IL-6R α , thus reducing IL-6 signaling that induces immune system activation^{5,16}. However, both tocilizumab and corticosteroids require high-dose, systemic administration, which does not localize the immunomodulators to the site of activated T cells. High-dose tocilizumab has been reported to lead to significant side effects, such as infections, reactivation of latent viral

infection, tuberculosis, and hepatotoxicity¹⁸. High-dose corticosteroids can lead to CAR-T cell attrition via apoptosis and inhibit antitumor efficacy of immune checkpoint blockade^{19,20}.

Therefore, to address this detrimental high-dosage problem, there are ongoing effort in the field to develop a system to enhance the localization of the immunomodulators to the site of activated T cells.

In addition to IL-6, a wide variety of cytokines including interferon gamma (IFN- γ), tumor necrosis factor alpha (TNF- α), and IL-1 are upregulated in patients with CRS. IFN- γ and TNF- α are notable cytokines produced by T cells, and they induce activation of macrophages and other immune cells, which further release proinflammatory cytokines^{21,22}. IL-1 is mainly produced by monocytes and has been reported to upregulate prior to IL-6 upregulation^{23,24}. Several studies have reported that the use of GM-CSF or IL-1R antagonist (IL-1Ra) can potentially treat CRS²³⁻²⁵, and these studies highlight the possibility of preventing CRS by inhibiting cytokine signaling other than IL-6 signaling.

In this thesis, we engineered CAR-T cells to “self-regulate” CRS through the secretion of various cytokine antagonists, which take the form of single-chain variable fragments (scFvs) derived from antibodies that target cytokines or their receptor proteins. These engineered CAR-T cells are designed to neutralize the CRS-related cytokine signaling at the site of T-cell activation, thus concentrating their effects at the location where they are most needed. We evaluated a panel of cytokine antagonists for different cytokines (IL-1, IL-6, IFN- γ , and TNF- α) for their potential as CRS modulators, and found CD19 CAR-T cells expressing an scFv derived from tocilizumab significantly reduced CRS-related toxicity while retaining effective anti-tumor function in a humanized mouse model of lymphoma. These results demonstrate potential of self-regulating CAR-T cells to prevent CRS *in vivo* without compromising their therapeutic efficacy.

Results

Cytokine antagonists derived from commercial drugs neutralize signaling of their intended targets

To evaluate a panel of cytokine antagonists for different cytokines (IL-1, IL-6, IFN- γ , and TNF- α) for their potential as cytokine release syndrome (CRS) modulators, we identified the sequence of multiple commercially available biologics and derived corresponding single-chain variable fragments (scFvs) (Table 3.1). The scFvs were linked to a second-generation anti-CD19 chimeric antigen receptor (CAR), with a 4-1BB co-stimulatory domain, via a T2A sequence (Fig. 3.1). The CAR molecule was confirmed to be efficiently expressed on cell surface and the scFvs were confirmed to be efficiently secreted by primary human T cells (Fig. 3.2a,b).

Table 3.1. List of cytokine modulators tested in this study.

Target Antigen	Modulator Constructs
IL-6R α	Tocilizumab scFv
IL-1R	IL-1Ra
TNF- α	Adalimumab scFv
TNF- α	Certolizumab scFv
TNF- α	Golimumab scFv
TNF- α	Infliximab scFv
IFN- γ	Emapalumab scFv

Next, to assess whether the scFv derived from tocilizumab could neutralize IL-6 activity, we expressed the panel of cytokine antagonists in a commercially available HEK cell line (HEK-Blue IL-6 Reporter Cells; InvivoGen) that expresses human IL-6 receptor and a STAT3-inducible secreted embryonic alkaline phosphatase (SEAP) reporter genes. IL-6 induces JAK/STAT3 activation. Upon stimulation with IL-6, the HEK cells expressing tocilizumab scFv showed significantly lower level of STAT3-induced SEAP secretion compared to the HEK cells

expressing other cytokine modulators (Fig. 3.3a), demonstrating that tocilizumab scFv inhibits IL-6 signaling.

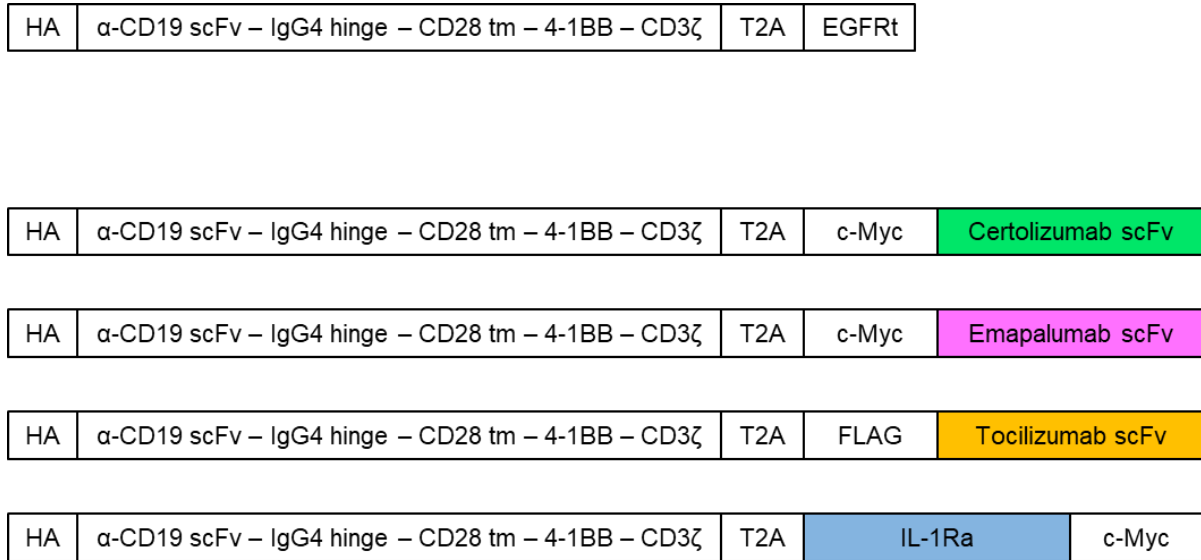


Fig. 3.1. Schematics of self-modulating CD19 CAR constructs. The CD19 CAR is composed of an N-terminal HA-tag as a transduction marker, an anti-CD19 scFv, an IgG4 hinge extracellular spacer, a CD28 transmembrane domain, a 4-1BB costimulatory domain, and a CD3 ζ signaling domain. The CAR is fused to a self-cleaving T2A peptide to either a truncated EGFR (EGFRt) or a cytokine modulator. All cytokine modulators are fused to an N-terminal c-Myc or FLAG-tag except IL-1Ra, which is fused to a C-terminal c-Myc tag instead for better protein production. The constructs were designed by Meng-Yin Lin.

Similarly, to investigate if the IL-1 receptor antagonist (IL-1Ra) co-expressed with CD19 CAR could inhibit IL-1 signaling, we expressed the panel of cytokine antagonist constructs in a commercially available HEK cell line (HEK-Blue IL-1 β Reporter Cells; InvivoGen) that express IL-1 receptor and a NF κ B and AP-1 inducible SEAP reporter genes. Upon stimulation with IL-1 β , the HEK cells expressing IL-1Ra showed significantly lower level of NF κ B and AP-1 induced SEAP secretion compared to the cells expressing other cytokine modulators (Fig. 3.3b), demonstrating that IL-1Ra inhibits IL-1 β signaling.

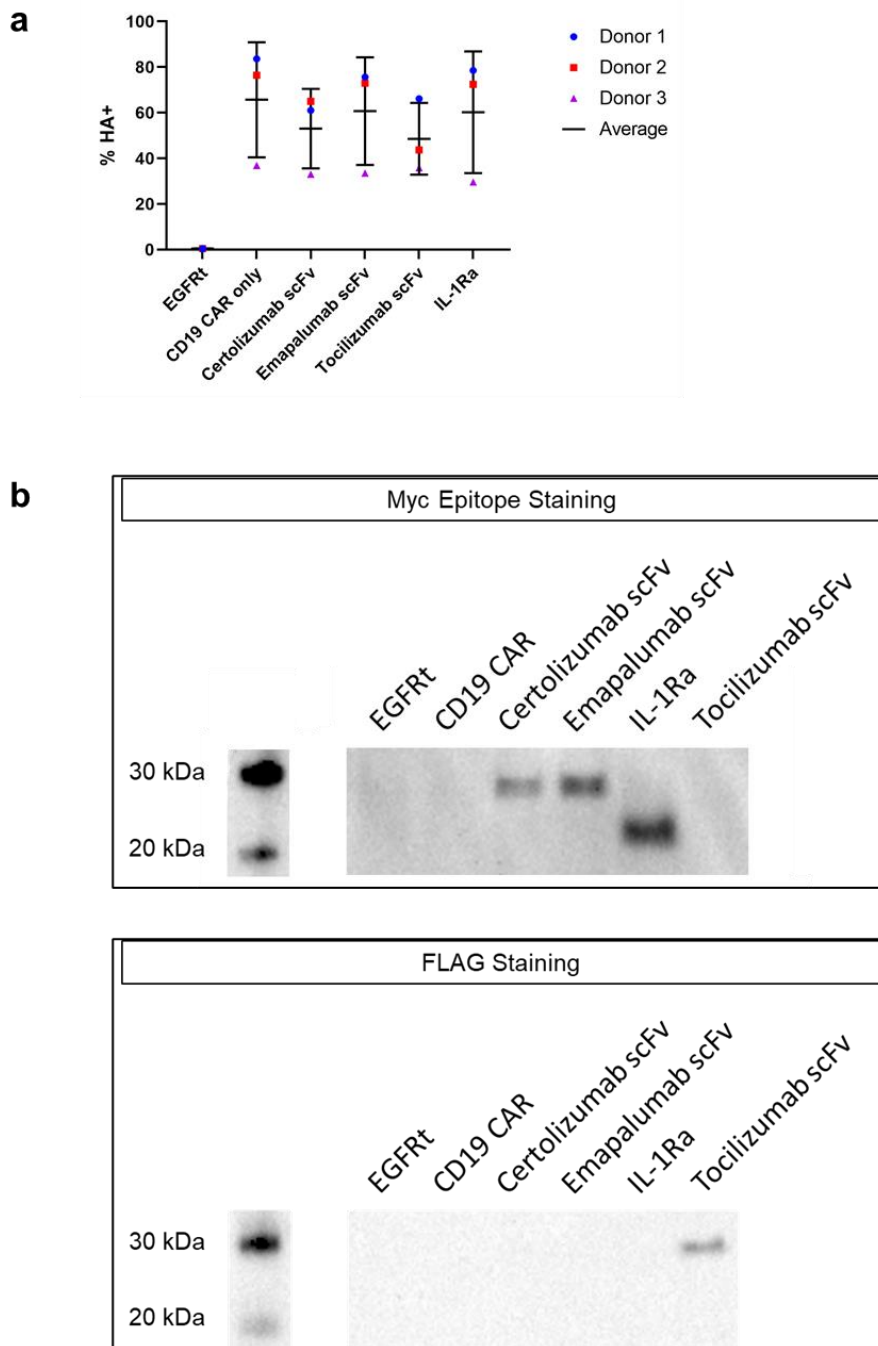


Fig. 3.2. CD19 CAR-T cells can robustly co-express cytokine modulators without compromising CAR expression *in vitro*. (a) Primary human T cells can efficiently co-express CD19 CAR with cytokine antagonists. CAR surface expression levels were quantified by surface antibody staining of HA-tag by flow cytometry. Values, means, and error bars indicating \pm SD from 3 donors are shown. (b) Primary human CD19 CAR-T cells express and secrete cytokine modulators. The secretion of the cytokine antagonists is detected by western blot on concentrated proteins from the T-cell culture supernatant. Certolizumab scFv is 29.9 kDa, emapalumab scFv is 30.6 kDa, IL-1Ra is 21.5 kDa, and tocilizumab scFv is 30.3 kDa in size.

The effect of anti-TNF- α scFvs on TNF- α signaling inhibition was assessed using a Jurkat cell line that expresses a NF κ B-induced enhanced green fluorescent protein (EGFP) reporter gene. Upon treating the Jurkat cells with varying concentrations of anti-TNF- α scFvs and stimulating with TNF- α , the Jurkat cells expressing either adalimumab scFv or certolizumab scFv, which are both anti-TNF- α scFvs, showed reduction in EGFP expression in a dose-dependent manner compared to untreated cells (Fig. 3.3c). This result depicted the efficacy of adalimumab- and certolizumab-derived scFvs in inhibiting TNF- α signaling. The other anti-TNF- α scFvs that were derived from infliximab and golimumab did not show significant reduction in EGFP expression. Also, between adalimumab and certolizumab scFvs, certolizumab scFv showed significantly lower TNF- α signaling inhibition than adalimumab scFv at the lowest dose. Thus, certolizumab scFv was chosen for further experiments as the anti-TNF- α antagonist.

Moreover, evaluation of supernatant cytokine level from co-culture of CD19 CAR-T cells co-expressing cytokine antagonists and CD19+ Raji cells showed negligible supernatant level of IFN- γ and TNF- α from CAR-T cells expressing emapalumab scFv and anti-TNF- α scFvs, respectively (Fig. 3.3d), demonstrating that both emepalumab scFv and anti-TNF- α scFvs bind to their intended target.

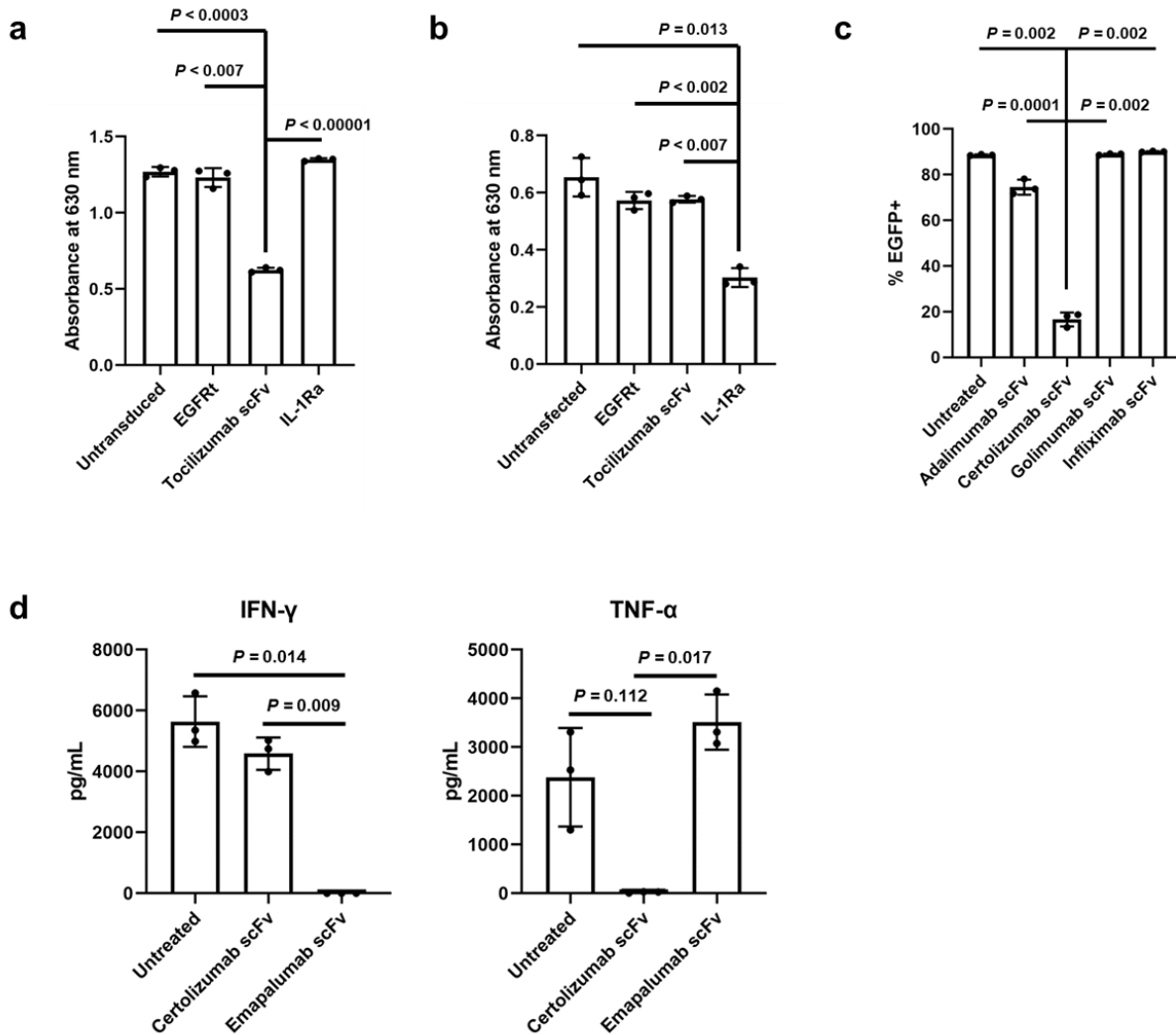


Fig. 3.3. Cytokine modulators neutralize signaling of their intended targets. (a) Tocilizumab scFv inhibits the activation of IL-6 pathway, which is quantified by the detection of STAT3-inducible secreted embryonic alkaline phosphatase (SEAP) secretion. (b) IL-1Ra inhibits the activation of IL-1 β pathway, which is quantified by the detection of NF- κ B/AP-1 inducible SEAP secretion. (c) Certolizumab scFv inhibits the activation of TNF- α pathway, which is quantified by the detection of NF- κ B inducible EGFP production, most effectively among the anti-TNF- α scFvs. (d) Both certolizumab scFv and emapalumab scFv bind to their intended cytokine targets: TNF- α and IFN- γ , respectively. Target cytokine binding by the cytokine antagonists prevents the detection of their target cytokine by the Cytometric Bead Array (CBA) assay. Values shown are the means of technical triplicate samples, with error bars indicating \pm standard deviation (SD). *P*-values were calculated by unpaired two-tailed Student's *t*-test with Bonferroni correction for multiple comparisons applied. Data for (c) and (d) were collected by Meng-Yin Lin.

CD19 CAR-T cells secreting cytokine modulators retain robust anti-tumor effector function *in vitro*

Although cytokines are the major contributor of CRS, they are also a critical player for T-cell mediated anti-tumor function. As such, we investigated whether the co-expression of cytokine modulators by CAR-T cells compromise the T cells' anti-tumor effector function. We first evaluated whether the co-expression of cytokine modulators affect T-cell expansion *ex vivo* without CAR-antigen stimulation and confirmed that the CAR-T cells retained normal *ex vivo* expansion (Fig. 3.4a). The T cells that co-express CD19 CAR and a cytokine modulator exhibited similar fold expansion post transduction compared to T cells that were either transduced with a mock construct or with only CD19 CAR construct.

We next assessed whether the secretion of cytokine antagonists would affect T-cell functions in the presence of CAR-antigen stimulation. The CD19 CAR-T cells secreting cytokine modulators were subjected to repeated antigen challenge to evaluate their antigen-stimulated proliferation and target-cell lysis, which are the two major functions of activated T cells besides cytokine production, upon multiple interactions with the target cells. For this, “self-regulating” CD19 CAR-T cells and Raji cells, which naturally express CD19 antigen, were co-incubated at a 1:1 effector-to-target (E:T) ratio, and the same number of target cells as the initial set-up was replenished every 2 days. The results showed that all CD19 CAR-T cells, regardless of co-expression of cytokine modulators, had comparable target-cell lysis and T-cell proliferation (Fig. 3.4b,c), demonstrating that the *in vitro* effector functions of CAR-T cells were not significantly affected by the co-expression of cytokine modulators.

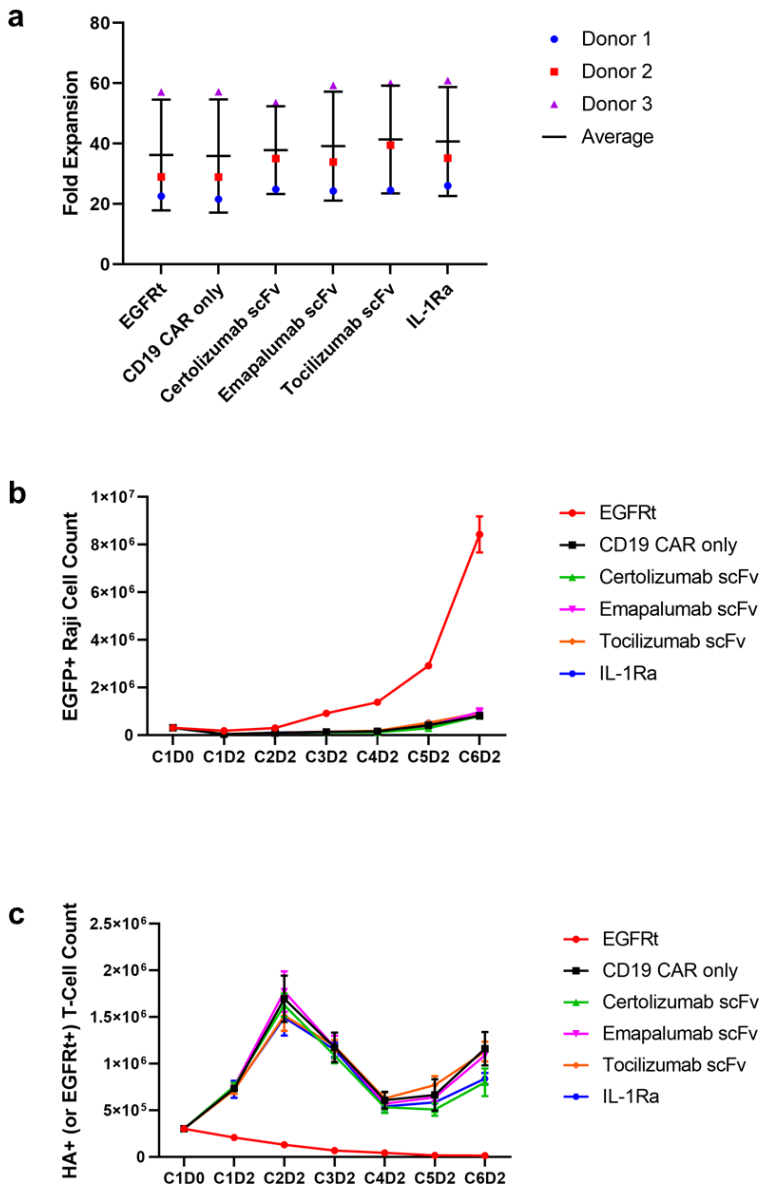


Fig. 3.4. Co-expression of cytokine modulators with CD19 CAR does not compromise T-cell function. (a) CD19 CAR-T cells secreting cytokine modulators retain normal *ex vivo* T-cell expansion. (b-c) CD19 CAR-T cells secreting cytokine modulators retain robust anti-tumor effector function of T cells upon repeated antigen challenge *in vitro*. Target-cell lysis is depicted in (b), and T-cell expansion is depicted in (c). CD19 CAR T cells were coincubated with Raji cells at a 1:1 E:T ratio and rechallenged every 2 days with the same number of fresh Raji cells as the initial challenge. ‘C#’ denotes the challenge number and ‘D#’ denotes the number of days post challenge. Values shown are the means of technical triplicate samples, with error bars indicating \pm SD.

CD19 CAR-T cells induce CRS in humanized NSG-SGM3 mice

To evaluate the ability of cytokine modulators to prevent CRS *in vivo*, we used humanized NSG-SGM3 mice. It had been reported that NSG-SGM3 mice reconstituted hematopoiesis more rapidly with more human B cells, T cells, monocytes, and other blood cells upon humanization with human hematopoietic stem and progenitor cells (HSPCs) compared to NSG mice²³. Since CRS is a systemic immune response that requires not only T cells but also other immune cells to amplify the cytokine signaling, we decided to apply the humanized NSG-SGM3 mouse model to establish as representative human immune system as possible in mice.

For this, NSG-SGM3 mice were humanized with human fetal liver HSPCs and engrafted with Raji cells about 3 weeks post humanization (Fig. 3.5a). To evaluate the difference between tumor progression-induced death, graft versus host disease (GvHD)-induced death, which is plausible with the presence of human T cells in murine system, and CRS-induced death, the mice were treated with PBS (i.e., untreated), mock-transduced T cells, or CD19 CAR-T cells about 7 days post tumor injection. Soon after the T-cell injection, mice treated with CD19 CAR-T cells showed relatively rapid decline in weight, temperature, and ultimately survival compared to those given either PBS or mock-treated T cells (Figures 3.5b-d). To verify that the CD19 CAR T-cell treated mice succumbed to CRS-induced toxicity, we assessed whether the CAR-T cell treated mice had higher serum human cytokine level than the untreated and mock-treated mice. As shown in Fig. 3.5e, CD19 CAR T-cell treated mice exhibited higher human inflammatory cytokine concentrations than both the untreated and mock-treated mice. This demonstrates that the humanized NSG-SGM3 mouse model effectively recapitulates CRS *in vivo*. Thus, we decided to use this mouse model to evaluate the effect of our panel of cytokine antagonists in preventing CRS.

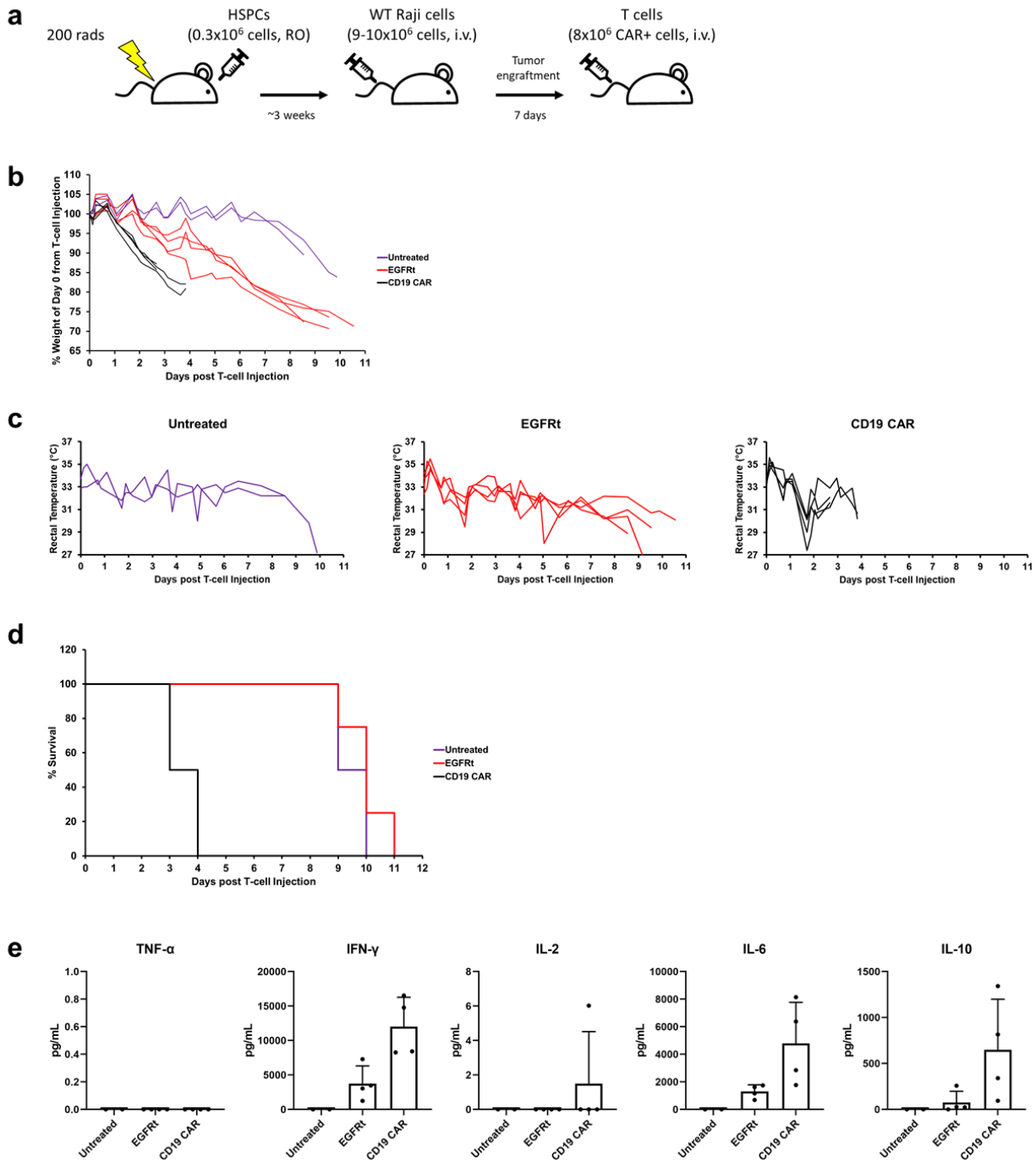


Fig. 3.5. CD19 CAR T cells induce CRS in humanized NSG-SGM3 mice. (A). Schematic of humanized animal study. NSG-SGM3 mice were sub-lethally irradiated (200 rads) and given 3×10^5 CD34⁺ HSPCs by retro-orbital injection for humanization. Humanization was confirmed when >20% of human cells were detected in peripheral blood. Humanized mice were engrafted with $9-10 \times 10^6$ Raji cells. Tumor-bearing humanized mice were treated with 8×10^6 EGFRt+ or

CAR⁺ T cells 7 days post tumor injection. For untreated mice, PBS was injected instead. CD19 CAR-T cells induce rapid decline in animal (b) weight, (c) temperature, and (d) survival. (e) CD19 CAR-T cell-treated mice had the highest cytokine levels. Rapid weight and temperature decline and upregulation of inflammatory cytokines like IFN- γ and IL-6 indicate that CD19 CAR-T cell-treated mice succumbed to CRS-related toxicities. Data for (a)-(e) were collected by Meng-Yin Lin.

CD19 CAR-T cells expressing tocilizumab scFv exhibit robust *in vivo* anti-tumor efficacy while reducing CRS-related toxicity

Following the schematic shown in Fig. 3.5a, NSG-SGM3 mice were humanized, engrafted with Raji cells, and treated with CD19 CAR-T cells co-expressing cytokine modulators. As expected, mice treated with CD19 CAR-T cells without cytokine modulator co-expression showed rapid decline in weight and temperature, which are the clinical signs shown to represent CRS-induced toxicity previously (Fig. 3.6a,b). However, mice treated with CAR-T cells co-expressing tocilizumab scFv or, to a lesser extent, IL-1Ra maintained relatively stable weight and temperature, demonstrating that tocilizumab scFv and IL-1Ra reduced CRS-related toxicity and helped the mice to exhibit prolonged survival (Fig. 3.6a,b). Furthermore, bioluminescence imaging revealed that all anti-CD19 CAR-T cells co-expressing cytokine antagonists cleared tumor (Fig. 3.6c). This shows that tocilizumab scFv secreted by the CD19 CAR-T cells ameliorated CRS and retained the CAR-T cells' anti-tumor effector function *in vivo*.

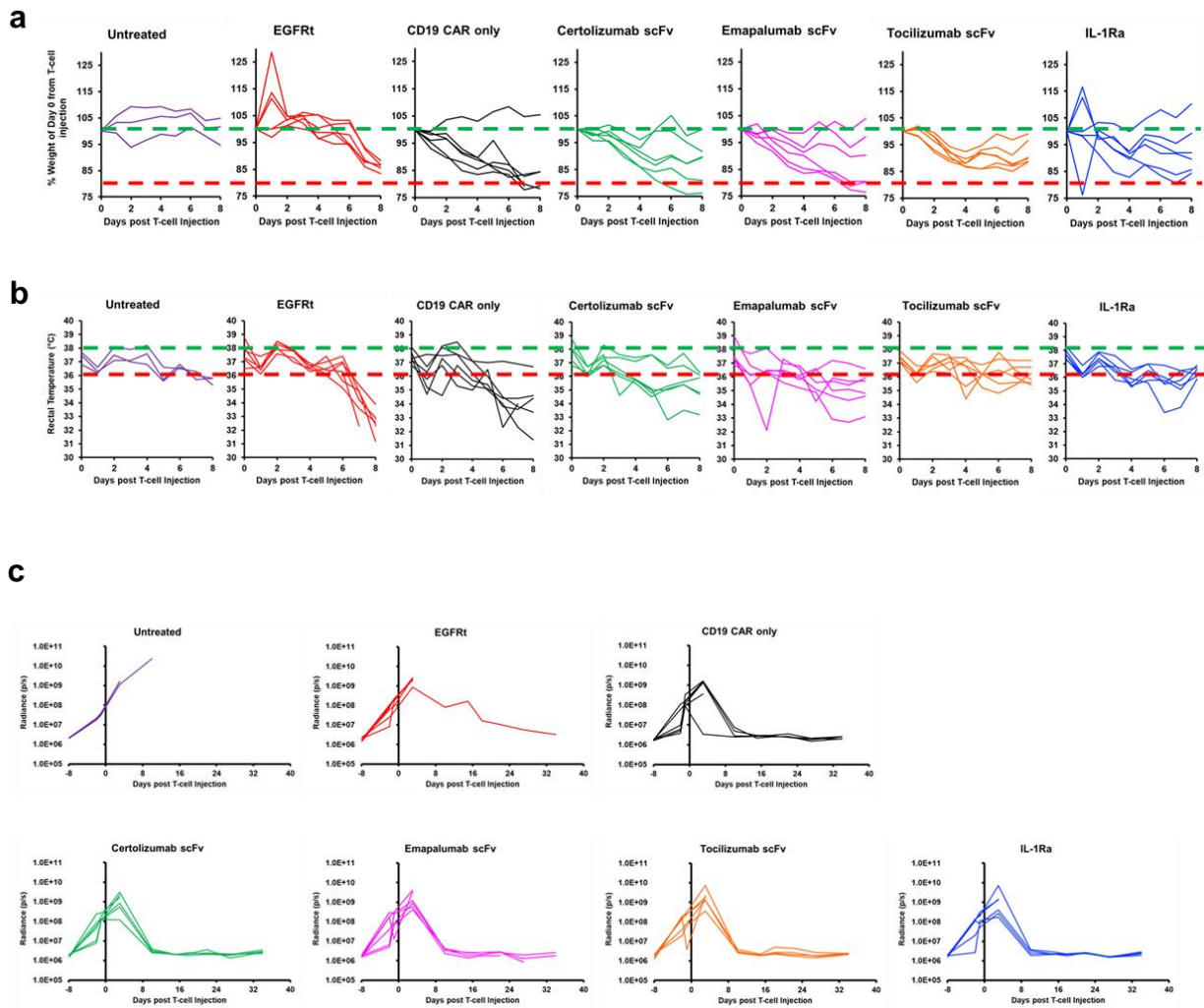


Fig. 3.6. CD19 CAR T cells expressing tocilizumab scFv exhibit robust *in vivo* anti-tumor efficacy while reducing CRS-related toxicity. Tocilizumab scFv rescue mice from (a) rapid weight loss and (b) rapid temperature loss, which were demonstrated to be symptoms of CRS-related toxicities from the previous figure (Fig. 3.5b,c). (c) CD19 CAR T cells co-expressing cytokine antagonists retain robust anti-tumor function *in vivo*. This indicates that co-expression of cytokine antagonists does not compromise T-cell function *in vivo*. The green dotted lines refer to healthy state, and the red dotted lines refer to detrimental state.

Tocilizumab scFv alters gene expression profile of CD19 CAR-T cells *in vivo*

To determine the effect of tocilizumab scFv on CD19 CAR-T cells in humanized mice, we performed single-cell RNA-sequencing (scRNA-seq) on human CD45⁺ cells isolated from

liver and spleen of mice treated with either only CD19 CAR-T cells or with CD19 CAR-T cells co-expressing tocilizumab scFv on day 8 post T-cell injection. Clustering analysis identified 16 clusters (numbered from 0 to 15; Fig. 3.7a). Evaluation of T-cell markers such as *CD3D* revealed that majority of the cells sequenced was T cells. Comparison of the UMAP plots of the control (CD19 CAR-T cells only, termed “CARonly” from hereafter) and tocilizumab scFv-treated (CD19 CAR-T cells co-expressing tocilizumab scFv; termed “Toci” from hereafter) samples revealed rise of a few distinct clusters (clusters 3, 4, 5, 6, and 9 from Fig. 3.7a) in the “CARonly” sample. These clusters expressed relatively high levels of cell cycle genes including *CDC20*, *TOP2A*, *PCNA*, and *MCM6* (Fig. 3.7b). Detailed-gene expression evaluation of these clusters revealed that these clusters represent cells at different cell cycle phases (Fig. 3.7c). Furthermore, gene set enrichment analysis (GSEA) was performed on overall data (i.e., all cells). The mountain plots exhibited that T cells from the “CARonly” sample were more metabolically active, as indicated by enrichment of gene sets for glycolysis and cell cycle (Fig. 3.7d). These results suggest that the presence of tocilizumab scFv alters gene expression profile of T cells *in vivo* by inhibiting IL-6 signaling pathway, which seems to diminish T cells’ metabolic activity.

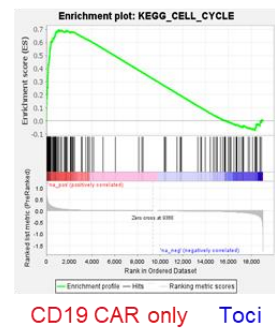
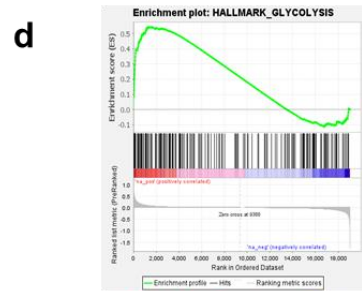
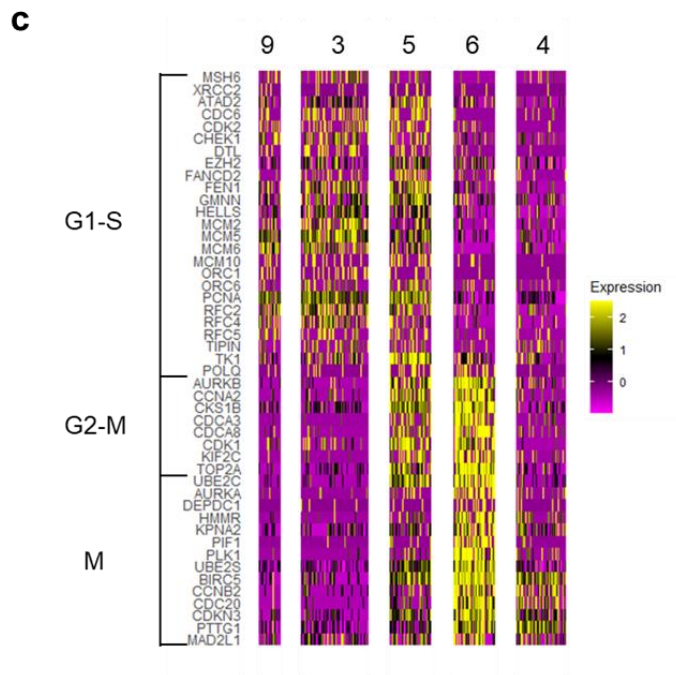
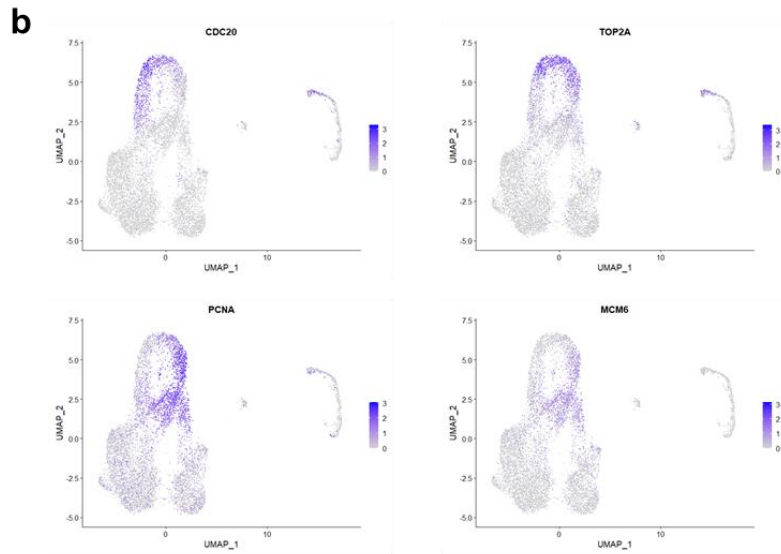
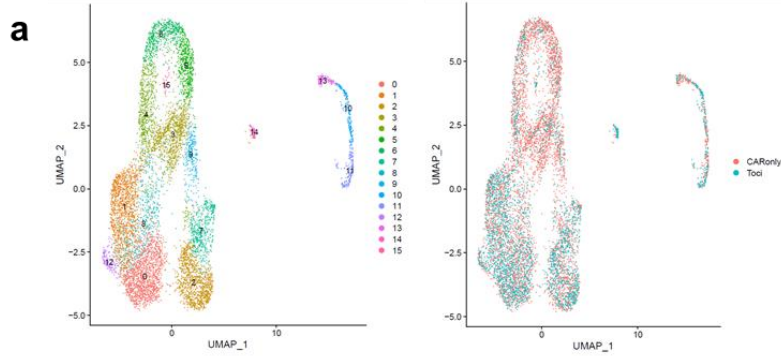


Fig. 3.7. Tocilizumab scFv alters gene expression profile of CD19 CAR-T cells *in vivo*. (a) UMAP plot of single-cell RNA-sequencing (scRNA-seq) data. Liver and spleen were harvested from the CD19 CAR T-cell treated humanized NSG-SGM3 mice on day 8 post T-cell injection. Then, CD45⁺ cells were isolated from the processed tissue samples and submitted for the scRNA-seq. Comparison of the UMAP plots of the “CARonly” control and “Toci” tocilizumab scFv-treated samples revealed rise of a few distinct clusters in the control sample. (b) Expression level of cell cycle-related genes in feature plots. (c) Expression level of cell cycle-related genes from clusters 3, 4, 5, 6, and 9 in a heat map. (d) Gene set enrichment analysis (GSEA) revealed that the “CARonly” sample is enriched for gene sets related to glycolysis and cell cycle. This suggests that the “CARonly” sample is more metabolically active than the “Toci” sample.

Discussion

Despite the success of CD19 CAR T-cell therapy for B-cell malignancies, the risk of severe treatment-related toxicities like CRS is one of the challenges that prevent the therapy from being the front-line option for cancer. Upon CAR T-cell activation, various cytokines like IL-1, IL-6, IFN- γ , and TNF- α upregulate and lead to development of systemic inflammatory immune response in patients. The anti-IL-6R α antibody tocilizumab and/or corticosteroid have shown clinical efficacy in treating CRS, but the treatment is only applied upon observation of CRS-related symptoms in patients. In this thesis, we developed an alternative approach to CRS management by engineering CAR-T cells that can lower CRS-related cytokine production automatically without compromising anti-tumor effector functions. In this way, CRS treatment would begin as soon as the T cells are injected and would prevent development of severe immune response before the patients exhibit CRS-associated symptoms. We found that CAR-T cells could co-express functional cytokine antagonists in the form of scFvs, which are derived from the commercially available biologics, while retaining anti-tumor functions. Using the humanized NSG-SGM3 mouse model, we provided actual recapitulation of CRS *in vivo* and showed prevention of CRS with the cytokine antagonists produced and secreted by T cells.

Moreover, in this thesis, we aimed to evaluate which of the CRS-related cytokine signaling pathways is the most critical signaling in terms of development of severe CRS. We evaluated functionality of cytokine antagonists targeting mainly four different CRS-related cytokine signaling (IL-1, IL-6, IFN- γ , and TNF- α signaling) *in vivo*, and identified that IL-6 signaling is the most important signaling of the four for the induction of CRS. The scRNA-seq data suggest that one possible mechanistic underpinning of how tocilizumab scFv rescues mice from CRS is by diminishing target antigen-stimulated T cells' metabolic activity.

It had been reported that neurotoxicity is often observed in patients with CRS. One possible cause of neurotoxicity is that while cytokines like IL-6 can cross the blood-brain barrier (BBB), antibodies like tocilizumab cannot cross the BBB due to their relatively large size. The cytokines that cross the BBB could then induce inflammatory response in brain. Despite the reports of CRS-associated neurotoxicity in clinics, our humanized NSG-SGM3 mouse model was not able to show any clinical symptoms related to neurotoxicity in mice, and this suggests a possible limitation to the animal model in studying CRS. However, we did detect CAR-T cells in the brain, so it could be possible that the CAR-T cells were able to produce cytokine antagonists in the brain and neutralized their target cytokines in the brain before the development of neurotoxicity.

Furthermore, as CRS has been observed in multiple CAR T-cell therapies with different targets like B-cell maturation antigen (BCMA), it remains necessary to test the self-regulating system in other CAR-tumor settings to evaluate the robustness of the system.

Materials and Methods

Plasmid construction

The heavy and light chain sequences of monoclonal antibodies, besides IL-1Ra, were connected with a 18-amino acid linker to generate cytokine antagonist scFv sequences. A second-generation CD19 CAR containing 4-1BB co-stimulatory domain was constructed and connected to the cytokine antagonist scFvs or IL-1Ra with a T2A sequence. All constructs were cloned in MSCV vector, which was a generous gift from Dr. Steven Feldman (National Cancer Institute).

Cell line maintenance

Raji cells (ATCC) were cultured in RPMI-1640 (Lonza) with 10% heat-inactivated FBS (HI-FBS; Life Technologies). Human embryonic kidney 293T (HEK293T) cells (ATCC) were cultured in DMEM (HyClone) with 10% HI-FBS. IL-1 β and IL-6 reporter HEK-Blue cells (InvivoGen) were cultured in DMEM with 10% HI-FBS. NF κ B-EGFP reporter Jurkat cells were a generous gift from Dr. Xin Lin (MD Anderson) and were cultured in RPMI-1640 with 10% HI-FBS.

Retrovirus production

HEK293T cells were seeded in 10-cm dishes at 3.5×10^6 cells in 9 mL of DMEM with 10% HI-FBS per dish and transfected by linear polyethylenimine (PEI). Sixteen hours post transfection, cells were washed with 3 mL of phosphate buffered saline (PBS; Lonza) without magnesium and calcium and supplemented with 8 mL of DMEM with 10% HI-FBS, 20 mM HEPES, and 10 mM sodium butyrate (Sigma-Aldrich). Eight hours later, cells were washed with PBS and supplemented with 7 mL of DMEM with 10% HI-FBS and 20 mM HEPES (DMEM-HEPES).

Viral supernatant was collected the following day and filtered through a 45- μ m filter (VWR). Seven milliliters of fresh DMEM-HEPES was added to the cells after the supernatant collection. The next day, another viral supernatant was collected, filtered, and combined with the first harvest. The final viral supernatant batch was stored at -80°C until further use.

Generation of CAR-expressing primary human T cells

Peripheral mononuclear blood cells (PBMCs) were isolated from healthy donor whole-blood (obtained from the UCLA Blood and Platelet Center) by using Ficoll density-gradient separation. CD14 $-$ /CD25 $-$ /CD62L $+$ naïve/memory (NM) T cells were subsequently isolated from the PBMCs using magnetism-activated cell sorting (MACS; Miltenyi) by first depleting CD14- and CD25-expressing cells and second enriching for CD62L-expressing cells. Isolated NM T cells were stimulated with CD3/CD28 T-cell activation Dynabeads (Life Technologies) at a 1:3 bead-to-cell ratio and transduced with retrovirus 48 and 72 hr post stimulation. Dynabeads were removed 7 days post stimulation. T cells were cultured in RPMI-1640 with 10% HI-FBS, 50 U/mL IL-2 (Life Technologies), and 1 ng/mL IL-15 (Miltenyi). Both IL-2 and IL-15 were supplemented every 2-3 days.

Flow cytometry

All flow cytometry experiments were performed with a MACSQuant VYB flow cytometer (Miltenyi). Flow data were analyzed and gated using FlowJo (TreeStar).

Tocilizumab scFv and IL-1Ra functionality assays

IL-1 β and IL-6 reporter HEK-Blue cells were seeded in 24-well plate at 5×10^4 cells/500 μ L/well and transfected by linear PEI. Twenty-four hours post transfection, 10 ng/mL IL-1 β (BioLegend) was added to the IL-1 β reporter cells and 10 ng/mL IL-6 (BioLegend) was added to the IL-6 reporter cells. Upon 18 hr post IL-1 β or IL-6 stimulation, levels of secreted embryonic alkaline phosphatase (SEAP) was monitored using QUANTI-Blue (InvivoGen).

Anti-TNF- α scFv functionality assay

NF κ B-EGFP reporter Jurkat cells were seeded in 96-well plate at 3×10^4 cells/200 μ L/well and incubated with designated concentration of TNF- α scFvs overnight at 37°C. In the following day, 10 ng/mL of TNF- α (Miltenyi) was added to each well. After 24 hr, EGFP reporter signal was evaluated by flow cytometry.

Repeated antigen challenge

Primary human T cells expressing CD19 CAR with or without cytokine antagonists were seeded in 24-well plate at 5×10^5 CAR+ T cells/1 mL/well and coincubated with Raji cells at 1:1 effector-to-target ratio. The total number of T cells for each construct was normalized with untransduced T cells. Every 2 days, number of T cells and remaining target cells were evaluated by flow cytometry. Also, 5×10^5 Raji cells were replenished to each well every 2 days after counting.

Isolation of CD34+ HSPCs from fetal liver

Fetal liver was obtained from the UCLA Gene and Cellular Therapy Core. The tissue was washed with PBS 3-4 times and dissected into 3-mm³ pieces in IMDM (Thermo Fisher). The dissected tissue solution was gently resuspended with a 10-mL syringe connected to a 16G-needle for 5-7 times to homogenize the tissue completely. Next, 250 U/mL collagenase (MP Biomedicals), 1200 U/mL hyaluronidase (Sigma-Aldrich), 150 U/mL DNase (Sigma-Aldrich), 1X pen/strep (Life Technologies), and 1X amphotericin (HyClone) were added to the homogenized tissue solution, and the solution was incubated in 37°C for 90 min. The tissue solution was filtered through a 100-µm cell strainer. Mononuclear cell isolation was performed using Ficoll density-gradient separation. After the isolation, CD34+ hematopoietic stem and progenitor cells (HSPCs) were enriched using magnetism-activated cell sorting (MACS; Miltenyi).

Humanized NSG-SGM3 mouse model with allogeneic HSPCs and adoptively transferred T cells

Six- to eight-week-old NSG-SGM3 mice (bred by the UCLA CFAR Humanized Mouse Core Laboratory) were sub-lethally irradiated (200 rads) with a Cesium-137 irradiator and injected 3×10^5 CD34+ HSPCs via retro-orbital injection. Three- or four-weeks post humanization, peripheral blood was collected via facial bleeding, and the cells in peripheral blood were stained for CD3, CD14, CD19, and CD45 and analyzed on a MACSQuant VYB flow cytometer (Miltenyi). Mice with more than 20% human cells were considered successfully humanized. Upon confirming humanization, $9-10 \times 10^6$ fluc-expressing Raji cells were injected via tail-vein injection. Seven days post tumor injection, 8×10^6 CAR+ T cells were injected via tail-vein

injection. Peripheral blood was collected 2 days and 11 days post T-cell injection. Weight and rectal temperature were assessed every day after T-cell injection. Tumor progression was monitored by bioluminescence imaging once or twice a week post tumor injection.

References

1. Xu, X. J. & Tang, Y. M. Cytokine release syndrome in cancer immunotherapy with chimeric antigen receptor engineered T cells. *Cancer Letters* vol. 343 (2014).
2. Brentjens, R., Yeh, R., Bernal, Y., Riviere, I. & Sadelain, M. Treatment of chronic lymphocytic leukemia with genetically targeted autologous t cells: Case report of an unforeseen adverse event in a phase i clinical trial. *Molecular Therapy* vol. 18 (2010).
3. Morgan, R. A. *et al.* Case report of a serious adverse event following the administration of t cells transduced with a chimeric antigen receptor recognizing ERBB2. *Molecular Therapy* **18**, (2010).
4. Teachey, D. T. *et al.* Cytokine release syndrome after blinatumomab treatment related to abnormal macrophage activation and ameliorated with cytokine-directed therapy. *Blood* **121**, (2013).
5. Lee, D. W. *et al.* Current concepts in the diagnosis and management of cytokine release syndrome. *Blood* **124**, (2014).
6. Kalos, M. *et al.* T cells with chimeric antigen receptors have potent antitumor effects and can establish memory in patients with advanced leukemia. *Science Translational Medicine* **3**, (2011).
7. Porter, D. L., Levine, B. L., Kalos, M., Bagg, A. & June, C. H. Chimeric Antigen Receptor–Modified T Cells in Chronic Lymphoid Leukemia. *New England Journal of Medicine* **365**, (2011).
8. Kochenderfer, J. N. *et al.* B-cell depletion and remissions of malignancy along with cytokine-associated toxicity in a clinical trial of anti-CD19 chimeric-antigen-receptor-transduced T cells. *Blood* **119**, (2012).

9. Brentjens, R. J. *et al.* CD19-targeted T cells rapidly induce molecular remissions in adults with chemotherapy-refractory acute lymphoblastic leukemia. *Science Translational Medicine* **5**, (2013).
10. Grupp, S. A. *et al.* Chimeric Antigen Receptor–Modified T Cells for Acute Lymphoid Leukemia. *New England Journal of Medicine* **368**, (2013).
11. Davila, M. L. *et al.* Efficacy and toxicity management of 19-28z CAR T cell therapy in B cell acute lymphoblastic leukemia. *Science Translational Medicine* **6**, (2014).
12. Kochenderfer, J. N. *et al.* Chemotherapy-refractory diffuse large B-cell lymphoma and indolent B-cell malignancies can be effectively treated with autologous T cells expressing an anti-CD19 chimeric antigen receptor. *Journal of Clinical Oncology* **33**, (2015).
13. Maude, S. L. *et al.* Chimeric Antigen Receptor T Cells for Sustained Remissions in Leukemia. *New England Journal of Medicine* **371**, (2014).
14. Ali, S. A. T cells expressing an anti-B cell maturation antigen chimeric antigen receptor cause remissions of multiple myeloma. *Blood* **128**, (2016).
15. Tanyi, J. L. *et al.* Possible compartmental cytokine release syndrome in a patient with recurrent ovarian cancer after treatment with mesothelin-targeted CAR-T cells. *Journal of Immunotherapy* **40**, (2017).
16. Chou, C. K. & Turtle, C. J. Assessment and management of cytokine release syndrome and neurotoxicity following CD19 CAR-T cell therapy. *Expert Opinion on Biological Therapy* vol. 20 (2020).
17. Rose-John, S. Il-6 trans-signaling via the soluble IL-6 receptor: Importance for the proinflammatory activities of IL-6. *International Journal of Biological Sciences* vol. 8 (2012).

18. Kroschinsky, F. *et al.* New drugs, new toxicities: Severe side effects of modern targeted and immunotherapy of cancer and their management. *Critical Care* vol. 21 (2017).
19. Shank, B. R. *et al.* Chimeric Antigen Receptor T Cells in Hematologic Malignancies. *Pharmacotherapy* vol. 37 (2017).
20. Tokunaga, A. *et al.* Selective inhibition of low-affinity memory CD8+ T cells by corticosteroids. *Journal of Experimental Medicine* **216**, (2019).
21. Shimabukuro-Vornhagen, A. *et al.* Cytokine release syndrome. *Journal for ImmunoTherapy of Cancer* vol. 6 (2018).
22. de Cesaris, P. *et al.* Tumor necrosis factor- α induces interleukin-6 production and integrin ligand expression by distinct transduction pathways. *Journal of Biological Chemistry* **273**, (1998).
23. Norelli, M. *et al.* Monocyte-derived IL-1 and IL-6 are differentially required for cytokine-release syndrome and neurotoxicity due to CAR T cells. *Nature Medicine* **24**, (2018).
24. Giavridis, T. *et al.* CAR T cell-induced cytokine release syndrome is mediated by macrophages and abated by IL-1 blockade letter. *Nature Medicine* **24**, (2018).
25. Sterner, R. M. *et al.* GM-CSF inhibition reduces cytokine release syndrome and neuroinflammation but enhances CAR-T cell function in xenografts. *Blood* **133**, (2019).